Monthly Scientific-Technical and Production Journal

The Paton WELDING JOURNAL

September 2001 # 9

English translation of the monthly «Avtomaticheskaya Svarka» journal published in Russian since 1948

The National Academy of Sciences of Ukraine
The E.O. Paton Electric Welding Institute of the NAS of Ukraine
International Association «Welding»

«The Paton Welding Journal»
is published monthly by the
International Association «Welding»

Promotion group:
V.N.Lipodaev, V.I.Lokteva
A.T.Zelnichenko (exec. director)
Translators:
S.A.Fomina, I.N.Kutianova,
T.K.Vasilenko
Editor
N.A.Dmitrieva
Electron galley:
I.V.Petushkov, T.Yu.Snegireva

Editorial and advertising offices
are located at PWI,
International Association «Welding»,
11, Bozhenko str., 03680,
Kyiv, Ukraine
Tel.: (38044) 227 67 57
Fax: (38044) 268 04 86
E-mail: journal@paton.kiev.ua

State Registration Certificate
KV 4790 of 09.01.2001

Subscriptions:
$460, 12 issues per year,
postage and packaging included.
Back issues available

«The Paton Welding Journal» Website:
http://www.nas.gov.ua/pwj

CONTENTS

We must work very hard for the sake of the future 2

SCIENTIFIC AND TECHNICAL

Ishchenko A.Ya., Lozovskaya A.V. and **Sklabinskaya I.E.** Physical simulation of heat processes in HAZ metal during welding aluminium-lithium alloys 4

Chigarev V.V. and **Shchetinin S.V.** Distribution of welding arc pressure 8

Cherepivskaya E.V. and **Ryabov V.R.** Pressure welding of dispersion-strengthened composite materials, containing silicon carbide particles (Review) 12

Labur T.M. Influence of isolated inner defects on fracture resistance of welded joints on aluminium-lithium alloys 19

Demidenko L.Yu. and **Onatskaya N.A.** Character of diffusion of carbon within the contact zone in thermal-press electro-hydropulse welding 22

Zyakhor I.V. and **Kuchuk-Yatsenko S.I.** Peculiarities of formation of friction welded joints between copper and aluminium 24

INDUSTRIAL

Kopilenko E.A., Pavlenko G.V., Samokhina T.I., Chmykhov N.V. and **Yumatova V.I.** Inspection /and testing of welding equipment serial-produced by Company «SELMA» and its conformity to requirements of DSTU ISO 9001–95 (fragments of the quality system) 30

Zamkov V.N. and **Akhonin S.V.** New methods for welding titanium and manufacture of unique large-sized titanium semi-finished products 33

BRIEF INFORMATION

Arsenyuk V.V. Interaction of copper with insoluble impurities under conditions of pulsed deformation in pressure welding 40

Brodovoj V.A., Gushcha O.I., Kuzmenko A.Z. and **Mikheev P.P.** Interaction of residual stresses in the zones of stress concentrators and fatigue cracks 42

ADVERTISING 44

WE MUST WORK VERY HARD FOR THE SAKE OF THE FUTURE

On July 12, 2001, Mr. G.M. Skudar, Chairman of the Board of JSC «Novo-kramatorsk Mechanical Engineering Plant» (Kramatorsk, Donetsk region), Director General of NMEP, held his traditional press-conference, in which he summed up the results of production and commercial activity during the first six months of the year 2001. Such meetings always go beyond the scope of the announced subjects. First of all, Mr. Skudar is a key figure for Kramatorsk, his words carry weight and his example is followed. Secondly, NMEP, as a city-making enterprise, is structured around the following principle «The plant is the city, and the city is the plant», and for Kramatorsk this is associated with development.

The main technical-economic results of the first six months are indicative of progressive development of NMEP and are 1.5 – 2.2 times higher, than last year's figures. Technical renovation programs have been funded for the sum of $22 mln, and 2002 development plan is currently been discussed at the plant.

The first six months had many milestones. This is setting up a shop area to make tools that will increase productivity by 1.5 to 3.0 times and will greatly improve product quality. A deep degassing unit has been commissioned and now very high quality steel is produced in NMEP. The accuracy of making teeth and gearing in the new gear-cutting area is higher, than the GOST requirements, and its products are in demand. From the beginning of the year 46 new machine tools have been put into operation in the mechanical shops. This means new jobs, new level of quality.

In addition, a technology of manufacturing rolls with a working layer of special grades of steel and cast iron is being mastered, that will widen the range of composite rolling rolls, including supporting rolls. Before the end of the year, upgrading four vertical furnaces will be completed to improve the quality of heat treatment and save energy carriers; an area for cutting up thick metal and another NC thermal-cutting unit will be commissioned, and a station for inert gas mixing will be set up.

Among the major events of the current year is completion of delivery to the Enakievo Metallurgical Works of an installation, including a «furnace-ladle» unit and a continuous-casting machine, that will be commissioned in November. A melting unit was shipped to Cherepovets «Severstal» Metallurgical Works. Sixteen shaft-sinking sets were shipped out, but unfortunately almost all of them went to Russia.

NMEP has made very substantial plans for the second half of the year. The outcome of several tenders, in which the plant participates, will be known. There is hope of Novokramatorsk people winning them. Shipments to France, Belgium, to Novolipetsk Metallurgical Works and «Severstal» are being considered; upgrading 5000 mill in Izhorsk Works and Mariupol Ilyich Works is under discussion, and renovation of «Krivorozhstal» and «Azovstal» is becoming a reality.

Right now the plant is introducing four investment projects under the programs of priority development territories, and their implementation will provide a new impetus for the plant development.

It was planned that in 2001 the salary at NMEP will be 1000 hrvn. at the minimum. In the second quarter the index was 1060 hrvn. The financial situation of the plant allowed not only maintaining holiday camps, but also starting repairs in the «Mashinostroitel» holiday home at the Azov sea, renovation of one building in the plants' rest home and renting a sanatorium in the Crimea for 10 years. Medical equipment is being purchased now for the medical institutions of the city. Equipment for 400,000 hrvn. will be supplied before the end of July, and the rest, for 600,000 hrvn., will delivered before the end of the year. In keeping with a recent decision of the Board of Directors and Managing Committee of the Stock Company, aid for the sum of 80,000 hrvn. will be provided to four city schools.

Rather good news for the Kramatorsk people is the fact, that despite a significant reduction of tax allocations to the city budget this year, the plant has transferred 10.7 mln hrvn. to the city treasury since the beginning of the year, this sum being by 2.2 mln hrvn. larger, than in the first half of last year.

The city pension fund has already received 28.3 mln hrvn. from NMEP this year, this being 1.8 times more, than the sum, transferred in the first half of last year. If the plant keeps up such a pace of

development, its deductions will amount to 80 % of all the retirement payment funds of Kramatorsk.

We are not just left to survive. The world reckons with us, we deliver products to industrialized countries, and upgrade our own production.

NMEP has been the plant of plants and will remain to be so. Tomorrow people will also drive cars, melt metal, make moulds and extract mineral resources.

One could think about Khartsizsk, for instance, that this city was doomed. But it turned out that the city had leaders and teams, who said «no» to falling into the precipice. Together with the pipe producers we created a line for fabrication of single-weld pipes of 1060 mm diameter. This is world-class development. Now a pipe of 1220 mm diameter is needed. Together with them, we very quickly developed a new mode and today the line produces the pipe of the required diameter, i.e. this is beyond the scope of the line preliminary design. In September a new pipe will have to go into production, namely of 800 mm diameter, because the plant has won a tender for delivery to Iran.

At present we have funded a contract for 11 mln hrvn. with Kramatorsk Machine-Tool Plant (KMTP) for delivery of four machine-tools. In addition, KMTP undertook to perform upgrading of eight Shkoda boring machines for NMEP, even though they did not do it before.

There is no doubt that our enterprises will live on. Certainly, a lot of hard work is required to create new jobs. This is a great effort, and a great need at the same time. It is the path followed by the entire world.

In conclusion, let me briefly dwell on the impressions that I have brought back from the European Community summit, held in Salsburg. Participation in it allowed seeing the tendencies in the Community development, and defining the role of Ukraine and NMEP in the world market.

Today the European community has changed the admission conditions for the candidate countries. First of all, elimination of all customs barriers in the goods traffic is stipulated. Secondly, it is the question of unrestrained migration of labour within Europe. Naturally, an Englishman will not come over to work in our mine, so it will mean our labour drifting over there. Third condition is free sale of land. On the other hand, retirement payments, social sphere and upbringing of children and overall progress are the internal affair of the country.

And if we do not take immediate measures in our country for a drastic improvement of labour productivity, introduction of new technologies, creation of new products and new social conditions, if we do not begin to markedly increase our production volumes, then we will let Europe tear us to pieces without offering any resistance at all. This was my chief conclusion from the summit.

So, today, whether we want it or not, Ukraine will never be isolated and independent of Europe. We manufacture just $600 of products annually per head. In France, Germany and Great Britain the product output is $25,000 per person. If we wish to have a worthy life under market economy, we must work very hard. And rely only on ourselves.

G.M. Skudar
Chairman of JSC Board
«Novokramatorsk Mechanical Engineering Plant»

PRESSURE WELDING OF DISPERSION-STRENGTHENED COMPOSITE MATERIALS, CONTAINING SILICON CARBIDE PARTICLES (REVIEW)

E.V. CHEREPIVSKAYA and **V.R. RYABOV**
The E.O. Paton Electric Welding Institute, NASU, Kyiv, Ukraine

ABSTRACT

Currently applied methods of producing dispersion-strengthened aluminium-based composite materials, reinforced with silicon carbide particles, are presented. The main physico-chemical and mechanical characteristics of these materials are given, and the current methods of joining dispersion-strengthened aluminium-based materials, as well as the problems arising in solid- and liquid-phase welding of these materials, are considered in detail.

Key words: *composite material, welding, aluminium matrix, reinforcer, particle, silicon carbide, aluminium carbide, decomposition, structure, composition, strength*

Aluminium alloys reinforced with high-strength ceramic particles of SiC with a high energy of interatomic bonds, are becoming widely accepted among the modern dispersion-strengthened composite materials (DSCM). A special feature of these materials is the fact that the matrix is their main load-carrying element, while the role of the reinforcing phase is mainly reduced to promoting the formation of a dislocation substructure in the processes of the alloy production, mostly at deformation and heat treatment, as well as to stabilising this substructure under the conditions of service. Use of aluminium as the matrix material is due to its extensive application in engineering, and the ability to control the properties of aluminium alloys by heat treatment.

These DSCM have a number of advantages compared to the matrix [1, 2]: increased strength (by 15 – 30 %) at room and medium (up to 350 °C) temperatures, rigidity (by 40 – 100 %), and wear resistance (2 – 3 times); lower linear thermal expansion coefficient (LTEC) (1.5 – 2.0 times). Compared to fibre-reinforced composite materials (CM), DSCM have isotropic properties, enable application of traditional kinds of plastic treatment (pressing, rolling, stamping) to make semi-finished products and items of them and have a significantly lower cost (5 – 10 times).

Used as matrix materials in DSCM are alloys AD33 (US analog 6061), AMg6 (1560), D16 (1160), alloy of Al–Cu–Mg system (2124), etc. The average level of mechanical properties for aluminium alloy based DSCM is as follows: σ_t = 400 – 600 MPa; $\sigma_{0.2}$ = = 300 – 470 MPa; δ = 3 – 6 %; E = 100 – 120 GPa, LTEC = $1.25 \cdot 10^{-7}$ degr^{-1} [3 – 5].

Use of a stable refractory compound, SiC, as the reinforcing phase, not interacting actively with the matrix material or dissolving in it right up to its melting temperature, enables preservation of the microheterogeneous structure and dislocation substructure, formed during deformation and heat treatment, up to submelting temperatures. This allows preserving the long-term performance of the composite right up to (0.90 – 0.94) T_{melt} of aluminium. SiC particles can be of different size, but the average diameter usually is in the range of 2 – 20 μm.

Properties of silicon carbide as a reinforcer. In the high-temperature region silicon carbide has a broad range of properties, namely refractory, antiabrasive, anticorrosion and strength [6 – 8]. Crystalline structure of silicon carbide is rather diverse: it is represented by a practically unlimited variety of polytypes, differing by the type of lattice symmetry and elementary cell parameters. All its types have binary tetrahedral structures. The source of such a complex polytypism is a kind of a dislocation-related mechanism (due to screw dislocations) of single-crystal growth.

Despite a multitude of silicon carbide polytypes, SiC filamentary crystals with not less than 99 % of the main phase of SiC β-modification, and commercial abrasive powders of green silicon carbide (α-SiC) are used as CM reinforcer.

Filamentary crystals are shaped as needles of 28 – 62 nm diameter with the specific surface of 20 – 45 g/m^2, commercial powders have a platelike shape and 1 – 40 μm diameter. Face roughness leads to the assumption of the powders being polycrystalline [9].

Silicon carbide of β-modification is formed at excess of silicon in the solidification medium, high cooling rates, nitrogen-rich atmosphere and higher pressure. Impurity phases, such as graphite, α-cristobalite, SiO_2, Fe_xSi_y, solid solution of silicon in α-Fe, $FeCl_x$ and products of their hydrolysis and oxidation, as well as α-SiC impurity have a negative influence on the mechanical properties of filamentary crystals of SiC β-modification. The impurity phase of graphite should be regarded as especially detrimental, as it

forms individual particles and conglomerates, as well as films on the surface of SiC filamentary crystals.

The best foreign manufacturers of silicon carbide provide 99.4 – 99.8 wt.% purity of filamentary crystals [10]. Its mechanical properties are as follows: σ_t = 20 GPa; E = 480 GPa, whereas SiC filamentary crystals produced in CIS countries have the following mechanical properties: $\sigma_t \geq 10$ GPa; $E \geq 500$ GPa with the main phase content of 99.2 – 99.9 wt.%.

The main disadvantage of silicon carbide filamentary crystals is their high cost, this hindering their application for CM manufacture or their broad acceptance by industry [11 – 13].

SiC abrasive powders, in addition to the main α-SiC phase, also contain free silicon and silicon, calcium, manganese, magnesium, aluminium and iron oxides and more complex oxide compounds [14]. Chemical analysis of SiC powders, applied for matrix reinforcement, showed that fine powders with a more developed surface, contain larger quantities of calcium and magnesium oxides. However, judging by the total content of silicon, made up by silicon from SiC, SiO_2 oxide, silicates and free silicon, coarse-grained powders are more contaminated with impurities than fine powders.

It was believed for a long time that application of commercial SiC powders as a reinforcer, requires preliminary cleaning, aimed primarily at removal of graphite and moisture, in view of the possible reaction of impurity graphite with aluminium in the weld pool and even during CM manufacture. However, electron diffraction analysis, conducted after preliminary treatment of powders by NaOH and HCl solutions [9], does not confirm the presence of free carbon in the initial powders. Powder oxidation in air at heating up to the temperature of 550 – 600 °C for 1.5 – 2.0 h, can be also performed to improve their wetting.

Silicon carbide is high-temperature and heat resistant. Both these indices are high for SiC with a minimal content of impurities, but the issue of its chemical stability is not yet completely studied.

Unfortunately, published data on silicon carbide properties are highly contradictory. According to [7], SiC melting temperature is higher than 2600 °C and even 2830 ± 40 °C [6, 8]. Furthermore, SiC is characterised by chemical stability: it is resistant to an oxidizing medium at the temperature up to 1500 °C, does not interact with nitrogen, is inert in hydrogen and carbon dioxide gas, resistant to many metallic and non-metallic melts. By the data of [15], however, SiC decomposition in contact with molten aluminium starts at the temperature of about 750 °C. Proceeding from thermodynamic concepts, the authors of [16] assumed that silicon carbide decomposition is not found below the temperature of 730 °C, but this statement is also inconsistent with practical data. References [17 – 19] report that the interaction between aluminium and silicon carbide starts already at the temperature of 660 °C and proceeds by the following reaction:

$$4Al + 3SiC \rightarrow Al_4C_3 + 3Si. \quad (1)$$

In addition to Al_4C_3, also Al_4SiC_4 and Al_8SiC_7 compounds can form in this system at the temperature above 1400 °C [15, 18, 19]. Silicon formed as a result of the reaction, dissolves in liquid aluminium solution. Therefore, controlling silicon dissolution and removal into the melt, allows influencing the progress of the reaction and, probably, even suppressing it.

LTEC for aluminium alloys is in the range from $24.1 \cdot 10^{-6}$ (AD33) up to $24.7 \cdot 10^{-6}$ (AMg6) $degr^{-1}$ (we will not consider LTEC of pure aluminium, equal to $28.7 \cdot 10^{-6}$ $degr^{-1}$, as it is practically not used as a matrix for CM manufacture). Based on various sources, LTEC of silicon carbide of β-modification is equal to $(5 – 7) \cdot 10^{-6}$ $degr^{-1}$, i.e. is approximately 4 times smaller, than that of aluminium alloys.

The density of aluminium alloys is ~2698, that of SiC — 3210 and Al_4C_3 — 2950 kg/m^3. Hardness of SiC is 24000 and that of Al_4C_3 — 19500 MPa.

Thus, if the ultimate strength of alloy AD33 (6061) is 320 – 380 MPa, in a CM on its base, containing 20 % SiC, σ_t amounts to 580 MPa (420 – 500 MPa on average). In D16 alloy ultimate strength is up to 410 – 460 MPa, and in a DSCM on its base with 18, 20 and 30 % SiC, σ_t is equal to 450 – 500, 520 – 540 and 580 – 600 MPa, respectively.

CM manufacture. In the general form, synthesis of materials, containing disperse particles (DP) of refractory compounds, includes preliminary preparation of the reinforcing phase; production of the melt of the selected matrix material; adding the reinforcing phase to it and achievement of its uniform distribution through the metal volume; pouring and solidification in a mould with subsequent hot working (heat treatment combined with extrusion or rolling) [10, 20 – 28].

A major obstacle to DSCM manufacture is poor wetting of the reinforcing phase particles by the aluminium melt. Therefore, the majority of the methods of DP addition to the aluminium melt, including preliminary preparation of the particles, are aimed, primarily, at reducing the contact angle of wetting of the particles by the melt. There are several variants of pretreatment of silicon carbide DP (Table 1).

Various methods of adding DP to the alloys have been currently developed, namely:

1. Production of a suspension of finely-dispersed particles directly in the metal, as a result of a chemical reaction of the melt with a special substance.

2. DP injection by an inert gas flow through an injection mould or using a plasma torch.

3. Mechanical mixing of the melt that is either in an overheated, or in a solid-liquid state to create a whirl in it, with simultaneous addition of reinforcing particles.

4. Use of vibration or ultrasound of a high intensity with superposition of mechanical stirring on the melt or without it, and subsequent injection of particles through a wave-guide-concentrator, immersed into the metal.

5. Forming briquettes (tablets) in simultaneous compacting of powders of the alloy base and DP with

Table 1. Variants of pretreatment of SiC reinforcing particles

Technology	*Purpose*	*Reference*
DP surface metallising, in particular cladding with nickel and copper	Improvement of wettability by changing Me–DP contact surface to Me–Me, prevention of DP interaction with the matrix melt	[26 – 28]
DP heat treatment, including IR heating in a non-oxidizing atmosphere	Degassing of DP surface to remove adsorbed gases, eliminating the overcooling effect	[21, 22]
Salt treatment of DP surface, also in a layer of flux, directly on the liquid metal surface or by sol-gel process	Improvement of wettability	[23 – 26, 29, 30]

their subsequent immersion into the melt and manual or mechanical stirring of the metal.

6. Mixing components of a special flux with the particles, applying the mixture on the liquid metal surface or placing it in a capsule under the melt surface and soaking up to completion of the reaction between the flux and the melt.

7. Melt filtering through a layer of the reinforcing phase directly during the mould filling up, using vacuum or high pressure.

Methods 2, 4, 7 require special, often expensive equipment and make the technology of DSCM manufacture more complicated, whereas variants 1, 3, 5 and 6 are less expensive and more readily adaptable to fabrication, and are widely accepted by industry [9].

Joining composite materials. It is known that the majority of metal-matrix CM are non-equilibrium systems, having a gradient of chemical potential on the particle–matrix interface, thus leading to interdiffusion of elements, and, hence, to formation of a zone of particle–matrix interaction. And even though element interdiffusion is necessary to provide their reliable adhesion, overdevelopment of this zone results in a degradation of the strength of the particles and the composite as a whole. Therefore, when joining composites, in particular, in welding, the temperature and time of contact interaction, should be thoroughly controlled. This is exactly the reason why until recently the item and the CM for it were developed as one package, without applying the traditional joining processes, this requiring additional cost [3, 31].

Composite welding involves difficulties, as high-temperature heating in welding can lead not only to loss of properties in the initial strengthened material, but also to weld embrittlement.

In order to select a more rational joining process, comparative analysis of structural changes in DSCM, caused by the impact of various welding heat sources should be conducted. It is necessary to evaluate the influence of different kinds of non-stationary heating in welding on the nature of particles decomposition, optimise the composition of filler materials that would not impair the properties of the welds or the welded joint as a whole, and compare the data on the joint mechanical properties.

Welding Al-based CM, reinforced with SiC particles [32 – 36] involves several problems: 1) decomposition of reinforcing SiC particles; 2) high viscosity of the weld pool; 3) difficult formation of a sound weld because of poor wetting of the particle surface with aluminium; 4) weld porosity.

In addition, there is one more problem in welding CM using filler wire. It is the absence of the base metal and filler mixing and, hence, lower strength of the welds, compared to that of the composite.

Therefore, the processes of DSCM joining in the solid state are especially effective, as in this case there are no problems with particle segregation or melt viscosity because of comparatively low temperatures of the process.

Diffusion welding. This commercial process of joining various similar and dissimilar metals and alloys has also become well-established in CM welding [37 – 44]. The welding process proceeds without the base metal melting, as a result of heating and compression of the parts being joined.

Diffusion welding of CM is characterised by applying intermediate metals or alloys in the form of inserts (foil), coatings and powder between the parts being joined or on one of the surfaces being welded. Foils with layers of other metal applied on them by vacuum deposition or gas-thermal spraying, can be also used [42, 43].

In [42] it was noted that the particle–particle interface formed in welding, makes the joint weaker. A schematic representation of welded joints produced using an insert and without it, is given in Figure 1. The schematic shows formation of new particle–matrix and particle–particle interfaces in the process of joining. Impact of high temperature and pressure leads to diffusion processes developing in the fusion zone, that are responsible for microalloying of this zone by intermediate metal elements and homogenising of their concentrations.

Diffusion welding of 2124 alloy based CM with 25, 30, 35 and 40 % volume fraction of reinforcing particles, was studied [40]. Samples had the form of discs of 25 mm diameter and 6 mm thickness. Prior to welding the surface was ground with abrasive paper and then degreased with acetone. Welding modes are given in Table 2.

Composite samples with 30 % volume fraction of the reinforcer were welded at T = 500 °C, t = 4 h, P = 10 MPa, 2 % deformation, using 2124 alloy as the insert. In this case, the welded joint ultimate strength was 110 ± 45 MPa, and under the same welding conditions, but without using the insert, it was 45 ± 15 MPa. Also considered are the chemical proc-

Table 2. Mechanical properties of composite welded joints produced in different welding modes

Reinforcer content, %	*Pressure, MPa*	*Sample deformation, %*	*Shear strength, MPa*
25	10	2	60 ± 10
30	10	2	45 ± 15
35	10	2	25 ± 10
40	10	2	35 ± 15
25	10	8	50 ± 10
25	12	14	45 ± 20
25	12	20	120 ± 5
30*	10	2	110 ± 45

*Welded using an insert of alloy 2124.

esses proceeding in the welding zone. Magnesium present in the alloy, reacts with aluminium oxide by the following reactions:

$$Al_2O_3 + 3Mg \rightarrow 3MgO + 2Al, \quad (2)$$

$$4Al_2O_3 + 3Mg \rightarrow 3MgAl_2O_4 + 2Al. \quad (3)$$

A more negative influence at the welding temperature of 500 °C is produced by the second reaction (with formation of $MgAl_2O_4$, that is located on the interface), but the oxidation process actually proceeds in an integrated manner.

Thus, the presence of magnesium and its chemical compounds lowers the shear strength of the welded joint, compared to the strength of joints on non-reinforced alloys of the same grade. Ultimate strength also depends on the volume fraction of silicon carbide. Use of an insert of an non-reinforced alloy improves the adhesion strength and the joint strength, respectively.

Reference [43] is a study of diffusion welding of overlap joints on 6 mm sheets of aluminium alloy 2124 (Cu — 4.4; Mg — 1.5; Si — 0.2; Fe — 0.3 wt.%; Al — balance), reinforced with SiC single-crystals, using inserts in the form of 50 – 150 μm foil of aluminium-lithium alloy 8090 (Cu — 1.2; Mg — 0.6; Si — 0.03; Fe — 0.07; Li — 2.4; Zr — 0.14 wt.%; Al — balance). Volume fraction of SiC was 12.5 %. Welding was performed at the pressure of $2.66 \cdot 10^{-2}$ Pa, temperature of 470 – 520 °C, compression force of 1.5, 3.0 and 6.0 MPa and compression time of 1 h. The influence of postweld heat treatment was also studied: soaking for 4 – 8 h at the temperature of 500 °C, cooling in iced water; some samples were subjected to artificial ageing at 190 °C for 16 h. For the welded joint, a maximum shear strength of 100 MPa was achieved, i.e. 90 % of this value for the base metal under the same heat treatment conditions. Welding was performed in the following mode: T = = 520 °C, P = 3 MPa, t = 1 h, but deformation was 43 %. When the compression pressure was lowered to 1.5 MPa, the ultimate shear strength dropped to 70 MPa, but the sample deformation did not exceed 30 %. The optimal mode of diffusion welding was as follows: T = 500 – 525 °C, P = 1 – 3 MPa, t = 1 h. Presence of lithium in the insert is favourable for the welding process, as it reacts with aluminium to form stable oxides, but with lower hardness and solubility

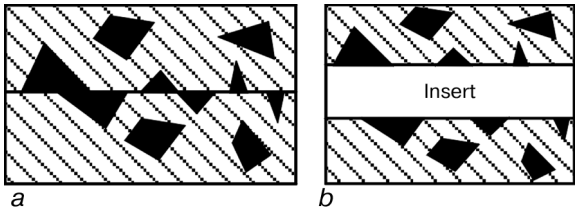

Figure 1. Schematic of a welded joint produced by diffusion welding without an insert (*a*) and with an intermediate layer (*b*)

under the studied welding conditions. Lithium diffusion into the base metal improves the strength of the base metal matrix and the phase along the matrix–SiC particle interface.

Influence of intermediate layers on the properties of welded joints of 8090 + 17 % SiC CM was studied in [44]. Alloy 8090 was used as the interlayer. Having studied the contact surface, the authors have come to the conclusion, that application of inserts results in a higher strength of the composite joints. Experiments on welding pure 8090 alloy, welding the composite with an insert and without it, were conducted for comparison. While the strength of 8090 alloy joint is on the level of 190 MPa, in welding CM without an insert, it amounts to just 100 MPa, whereas a welded joint of CM with an insert has the strength of 150 MPa.

Reference [37] is a study of a CM, consisting of a matrix of aluminium alloy 2618 (Cu — 2.27; Mg — 1.07; Fe — 1.55; Mn — 0.01; Zn, Ti — 0.02 wt.%), reinforced with SiC particles in the amount of 15 vol.%. A rod of 45 mm diameter was produced by extrusion, so that SiC particles had a certain orientation in the direction of the extrusion. Discs of 3 mm thickness were cut off the rod, which were cut up into plates of square shape, that were cleaned with emery paper, polished with diamond paste and degreased with acetone. Diffusion welding of samples was performed either directly (without an insert), or with an insert of Al–Mg alloy (Mg — 4.31; Si — 0.31; Fe — 0.57; Mn — 0.23 wt.%) in the form of 20 μm thick foil, or with a layer of silver coating 0.25, 0.50 and 1.00 μm thick, on each side of the samples. Welding was carried out in argon, with sample heating at the rate of 20 °C/min up to the temperature of 500 °C. Without the insert, with application of foil and silver coating welding pressure was 10 – 25, 10 – 20 and 10 – 15 MPa, respectively, with the compression ratio of 27.0 – 58.0, 25.0 – 53.0 and 21.3 – 36.3 %. A joint without a clearly-defined interface at the welding time of 1 h and up to 25 MPa pressure, can be produced without using the insert. When foil is used (t = 1 h, P = 20 MPa) a joint with a hardly visible interface and with SiC particles on its line is formed. Compression ratio is rather high (53 %). In the case a silver coating is used, a sound joint (without a visible interface) is formed at the coating thickness of 0.5 μm, welding time of 2 h, compression force of 15 MPa and compression ratio of 36.3 %. In order to reduce the compression ratio, the authors recommend the compression to be performed in two stages, namely under pressure and without it. Then welding can be performed at the compression ratio of 20 %.

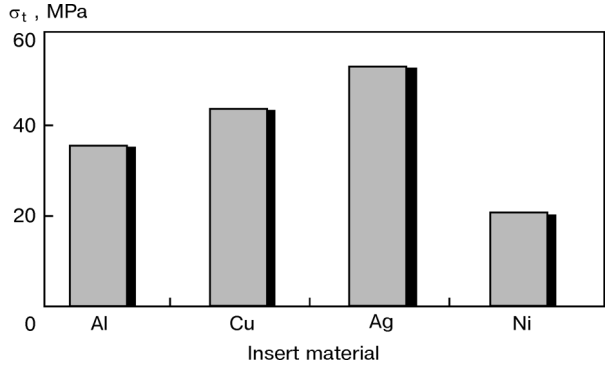

Figure 2. Ultimate strength of welded joints of 6061 + 20 % SiC CM, made by diffusion welding with inserts of different materials

In study [38] experiments were conducted on diffusion welding of a CM of 6061 + 20 % SiC filamentary crystals. A butt joint design was selected for experiments. The surfaces to be joined were ground with abrasive paper, then cleaned and etched to remove surface contamination and oxide films. To produce an acceptable joint, samples were joined through an intermediate layer of foil. Inserts of different materials were used to provide the maximal strength and chemical homogeneity of the joints. Diffusion welding parameters are given in Table 3. The joining process was conducted under a vacuum of $133.3 \cdot 10^{-2}$ Pa. All the joints with an insert were characterized by a good contact, atom mobility being sufficient for formation of a diffusion layer of foil material. It is noted that the diffusion layer of nickel is wider, than that of inserts of other materials. This is attributable to the close atomic radii of nickel and aluminium (R_{Al} = = 0.140, R_{Ni} = 0.125 nm). In the absence of an intermediate layer, a large number of discontinuities were found in the joint, as filamentary crystals prevent aluminium diffusion. With copper inserts, the quality of the produced joints is satisfactory. Dependence of welded joint ultimate strength on the insert material is shown in Figure 2, σ_t of welded joints being much lower, than that of the base metal.

The «corrosion aspect» of applying inserts in diffusion welding should be also noted. In order to achieve a high corrosion resistance of the joint, the interlayer composition is usually selected to have close electrochemical properties. In view of the fact that the metals being welded and the intermediate layer have different chemical composition, and the intermediate layer has a stationary electrode potential relative to the metals being welded, the corrosion resistance of the welded joint is increased [45]. Impact of high temperature and pressure results in development in the welding zone of processes that homogenize element concentration on the interface of the materials being welded, thus providing a smooth change of the electrode potential in the welding zone and reduction of corrosion localizing. Change of electrochemical properties caused by a positive potential shift, leads to an increase of the welded joint corrosion resistance over the entire cross-section.

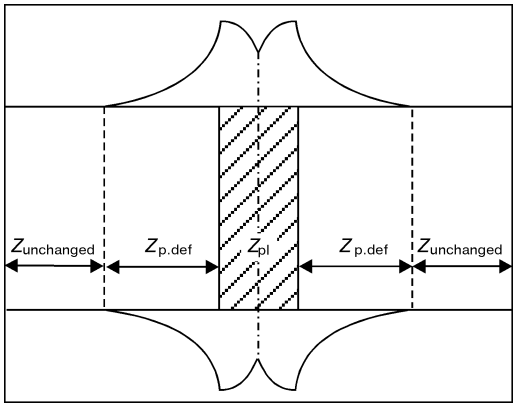

Figure 3. Zones of a welded joint made by friction welding

Table 3. Modes of diffusion welding of 6061 + 20 % SiC CM

Interlayer	*Welding temperature, °C*	*Welding pressure, MPa*	*Welding time, min*
Al	550	8	30
Ni	580	12	20
Cu	520	6	15
Ag	550	12	20
Without insert	580	15	30

Thus, diffusion welding is applicable to joining Al-based DSCM, but in order to achieve the maximal strength, it is necessary to select an appropriate combination of the insert material and welding mode.

Friction welding. Friction welding is one of the promising methods of composite joining, that has attracted a lot of attention lately. This is due to the absence of the problems of weld pool viscosity and the reaction between the matrix material and the reinforcer.

All its variants are applied for CM welding, namely rotation, inertia and linear [3, 5]. It is noted that high rates of relative displacement and the released heat break up the reinforcing particles near the contact boundary, and a loss of hardness is found in the HAZ. For joints of 2618 + 14 % SiC DSCM, made by rotation welding, the following welding modes were found to be optimal: rotation velocity 950 rad/min; rotation force 20 t; forging force 30 t; «hot» upset 4 mm; total upset 8.5 mm; welding time 1.4 s. Full postweld heat treatment (quenching and ageing) provides strength properties of the joints, close to those of the base material.

According to the data of [3], friction welding permits joining composites produced by casting and pressing. Figure 3 shows the shape of the welded joint of 45 mm diameter rods of 2618 + 14 % SiC DSCM. The authors of [46] separate the welded joint zone into the zone of complete plastic deformation Z_{pl} and zone of partial deformation $Z_{p.def}$.

Reference [46] is a study of the structure and mechanical properties of the joints made by inertia friction welding on aluminium alloy 8009 (Fe — 8.5; Si — 1.7; W — 1.3 wt.%), reinforced by 11 vol.% of SiC particles. Hot deformation results in formation of a homogeneous structure with a uniform distribution of SiC particles along the rod butt joint. No traces of a chemical reaction between SiC and the matrix were detected in the joint; in some cases cracking of large SiC particles was found in the weld and base metal. Mean values of Knoop microhardness in the heat-affected and deformation impact zone and in

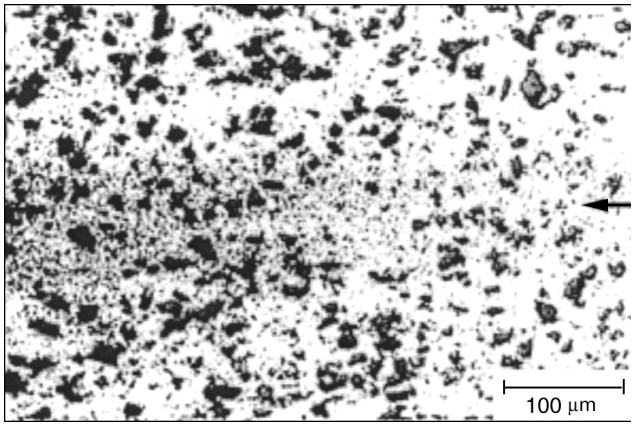

Figure 4. Microstructure of the zone of a joint made by friction welding. The arrow shows the joint line (reduced by 3/5)

the base metal are quite close. No weak zones were found in the vicinity of the weld; σ_t of the welded joint is more than 90 % of this value for the base metal, this being in agreement with the results of microhardness measurement. In tensile testing the joints always failed on the outer edge in the heat-affected and deformation impact zone; the matrix and the weld metal failed in the ductile mode, and the SiC particles in the brittle mode. Joint microstructure and hardness distribution over the cross-section of a sample, made by friction welding, are shown in Figures 4 and 5, respectively.

Resistance spot welding. Resistance spot welding has been accepted as a promising method of joining DSCM components to structural elements [32]. Weldability of the joints was evaluated on technological samples of the same DSCM grade, as well as for combinations of DSCM with aluminium alloy D16. D16 + 20 % SiC DSCM samples 2.0 mm thick were used for investigations. Sample surface was prepared for welding by chemical etching and mechanical cleaning. Such an operation does not practically differ from similar treatment of aluminium alloys. Welding was conducted in a capacitor-type machine MTK-75, using electrodes of alloy Br.KD1. Welding parameters were determined on samples by individual selection of the mode, as for aluminium alloys of D16 type.

The criteria for evaluation of the quality of spot welding of DSCM of D16 + SiC system, were the data of technological samples, micro- and macroanalysis, investigation of the mechanical properties of samples, as well as radiography of weld spots. The results of studying the welded joints are given in Table 4. It is found that the diameter of the weld spot cast zone in welding DSCM samples to each other and to a sample of aluminium alloy corresponds to the generally accepted dimensions for welding aluminium alloys of D16 type.

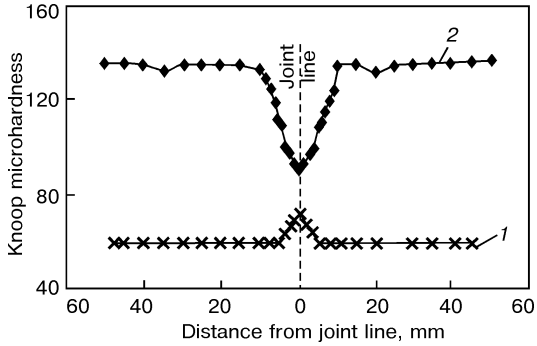

Figure 5. Microhardness distribution across the sample cross-section: *1* — quenching and artificial ageing in a mode, providing an improved fracture toughness and corrosion resistance; *2* — quenching and full artificial ageing

The presence of a cladding layer in a DSCM blank, does not significantly influence the weldability and strength in similar material combinations.

In tensile testing of DSCM sample joints, all the fractures had the form of a shear, and in pull testing, partial separation of the outer aluminium cladding from the material being welded was observed.

No tears along SiC particles were found in the fracture of the weld spot nugget (with particle size < 10 μm). Fracture surface that is of a brittle macroscopic nature, consists of pits. Surface studies demonstrated that SiC particles are non-uniformly distributed in the fracture sites, and in some regions of the spot nugget, clusters of SiC particles or discontinuities, nucleating at the particles, are found. Radiographic studies of individual samples revealed minor defects (porosity) located in the center of the spot cast zone.

Weld spot shear strength is somewhat higher for joints of sheet blanks of CM combinations, than in a similar joint of sheet blanks of alloy D16. This is, probably, related to the fact, that CM rigidity is higher, therefore, the probability of a weld spot failing through separation, becomes smaller.

Resistance welding was applied for sheets of alloy 6082 + 20 % SiC CM. The composition of alloy 6082 was as follows, %: Si — 0.7 – 1.3; Fe — 0.5; Cu — 0.1; Mn — 0.4 – 1.0; Mg — 0.6 – 1.2; Cr — 0.25; Zn — 0.2. However, a pronounced segregation of SiC particles was noted [4]. Use of capacitor-type welding for DSCM is also possible [47]. Finally, the process of magnetically-impelled arc butt welding was also used for joining pipes of DSCM of alloy 2124 + 25 % SiC [3, 5].

Thus, among the currently used solid-phase welding processes diffusion welding, performed with inserts, provides the welded joint strength not exceeding 50 – 60 % of that of the initial DSCM. In some cases application of heat treatment can increase the welded joint strength up to 90 % of that of the base

Table 4. Properties of welded joints on samples of DSCM D16 + 20 % SiC and aluminium alloy D16

Material	*Weld spot diameter, mm*	*Depth, %*				*Weld spot shear strength, MPa*	*Weld spot pool strength, MPa*
		Penetration		*Indentation*			
		DSCM	*D16*	*DSCM*	*D16*		
DSCM + DSCM	6 – 7	60	85	10	15	250 – 280	160 – 190
D16 + DSCM	6 – 7	60	–	10	–	260 – 300	170 – 200
D16 + D16	6	–	30 – 80	–	15	240 – 260	150 – 180

metal. However, the influence of heat treatment has not yet been completely studied. It is necessary to carry on investigations not only in the field of improvement of diffusion welding technology, but also studying the influence of heat treatment on the properties and microstructure of DSCM welded joints.

Friction welding yields somewhat better results (σ_t up to 90 % of this value for the base metal). Both the methods are applicable for joining rods, pipes and other bodies of revolution. Therefore, the new process of friction stir welding is quite promising for welding Al-matrix DSCM. Good results are achieved with resistance spot welding.

Finally, in the authors' opinion, it is necessary to improve also the technologies of composite materials manufacture, so as to minimise the possible defects in the initial material, such as pores, slag inclusions, particles agglomeration, etc.

REFERENCES

1. Bondarev, B.I., Polkin, I.S., Romanova, V.S. (1990) Composite materials based on aluminium alloys reinforced with SiC particles. In: *Proc. of Int. Conf. on Promising Tendencies in Aircraft Materials*. Moscow.
2. Bondarev, B.I., Polkina, I.S., Romanova, V.S. *et. al.* (1991) Status and prospects for development of manufacturing aluminium-based composite materials, reinforced with ceramic particles. In: *Composite materials*. Kyiv: PWI.
3. Ellis, M.B. (1996) Joining Al-based metal matrix composites — a review. *Mater. and Manufacturing Proc.*, **1**, 45 – 66.
4. Ellis, M.B., Gittos, M.F., Thereadgill, P.P. (1994) Joining aluminium-based metal matrix composites. *Materials World*, **8**, 415 – 417.
5. Lundin, C.D., Danko, J.C., Swindman, C.J. (1990) Fusion welding of SiC-reinforced aluminium alloy 2024. In: *Proc. of Conf. on Recent Trends in Welding Science and Technology*. AMS Int. Materials Park.
6. (1966) *Silicon carbide (structure, properties and applications)*. Ed. by I.N. Frantsevich. Kyiv: Naukova Dumka.
7. Dobrolezh, S.A., Zubkova, S.M., Kravets, V.A. *et al.* (1963) *Silicon carbide*. Kyiv: Gostekhizdat Ukr.SSR.
8. Khenish, G., Roy, R. (1972) *Silicon carbide*. Moscow: Mir.
9. Chernyshova, T.A., Kobeleva, L.I., Shebo, P. *et al.* (1993) *Interaction of metallic melts with reinforcing fillers*. Moscow: Nauka.
10. Kawabe, A., Oshida, A., Kobayashi, T. *et al.* (1999) Fabrication process of metal matrix composite with nanosize SiC particle produced by vortex method. *J. Jap. Inst. of Light Metals*, **4**, 149 – 154.
11. Fujita, Y. (1989) Composites on the basis of alloys of aluminium reinforced ceramic thready chips and fibers of short kerf. *J. Iron and Steel Inst. of Jap.*, **9**, 102 – 111.
12. Morimoto, K. (1991) Composites on the basis of alloys of aluminium, reinforced thready chips from SiC. *Joining Assembling Automation*, **11**, 22 – 25.
13. Fujita, Y. (1989) Composites: aluminium alloys, hardened by ceramic thready chips and short fibres. *J. Iron and Steel Inst. of Jap.*, **9**, 1516 – 1525.
14. Chernyshova, T.A., Bolotova, L.K., Kobeleva, L.I. *et al.* (1999) Arc welding of discretely reinforced composite material of Al–SiC system. *Fizika i Khimiya Obrab. Materialov*, **4**, 57 – 62.
15. Iseki, T., Kameda, T., Maruyama, T. (1984) Interfacial reactions between SiC and aluminium during joining. *J. Mater. Sci.*, Vol. 19, 1632 – 1638.
16. Hill, J.F., Wilkinson, S.W., Fenn, R. (1997) Fusion welding of an aluminium matrix/SiC reinforced MMC. *Int. J. for the Joining of Materials*, **2**, 61 – 65.
17. Chernyshova, T.A., Korzh, T.V., Kobeleva, L.I. (1997) Products of interaction in aluminium alloy/SiC particles composition, produced by liquid-phase methods. *Fizika i Khimiya Obrab. Materialov*, **3**, 54 – 61.
18. Han, L., Meg, Q.C., Zhang, J. *et al.* (2000) Resistance brazing of SiC/2024Al composite. *Acta Metallurgica Sinica (English Letter)*, **1**, 212 – 216.
19. Viala, J.C., Fortier, P., Bouix, J. (1990) Stable and metastable phase equilibria in the chemical interaction between aluminium and silicon carbide. *J. Mater. Sci.*, Vol. 25, 1842 – 1844.
20. Esaulov, I.V., Stepanov, B.I., Kitajgorodsky, Yu.I., *et al.* (1972) *Experience of application of ultrasonic degasifier UZD100 for commercial-scale production of dispersion-strengthened aluminium alloys with oxide and carbide particles*. Moscow: Mashinostroyeniye.
21. Serebrinsky, E.I., Gorykin, I.V., Zolotarevsky, Yu.S. *et al. Master alloy*. USSR author's certificate **538045**, Int. Cl. C 22 C 21/00. Publ. 05.11.76.
22. Serebrinsky, E.I., Vladimirov, Yu.I., Zolotarevsky, Yu.S. *et al. Master alloy*. USSR author's certificate **678079**, Int. Cl. C 22 C 35/00. Publ. 05.08.79.
23. Mikhalenkov, K.V., Mogilatenko, V.G. (1996) Production of aluminium-base dispersion-strengthened and composite materials. *Protsessy Litia*, **2**, 49 – 63.
24. Mikhalenkov, K.V., Chernega, D.F., Mogilatenko, V.G. *et al.* (1996) On refractory compound assimilation by liquid aluminium alloys. *Ibid.*, **1**, 3 – 10.
25. Soloviev, V.P., Amanzholov, Zh.K. (1979) Advanced technologies of aluminium alloy strengthening. In: *Proc. of 2nd Rep. Sci.-Techn. Conf. on Non-metallic Inclusions and Gases in Casting Alloys*. Zaporozhje.
26. Chernega, D.F., Mikhalenkov, K.V., Mogilatenko, V.G. *et al.* (1995) Application of new fluxes for strengthening treatment of aluminium alloys. *Protsessy Litia*, **3**, 82 – 88.
27. Lloyd, D.J. (1989) The solidification microstructure of particulate reinforced aluminium/silicon carbide composites. *Composite Sci. and Techn.*, Vol. 35, 159.
28. Lloyd, D.J., Lagace, H., McLeod, A. *et al.* (1989) Microstructural aspects of aluminium/silicon carbide particulate composites produced by a casting method. *Mater. Sci. and Techn.*, Vol. 5, 73 – 77.
29. Edgar, E., Cudio, E., Manfred, M. *Preparation of a composite material*. Pat. **1194584** FRG. Publ. 1973.
30. Edward, P., Arnold, A. *A method to produce a composite material*. Pat. **1431882** Great Britain. Publ. 1981.
31. Jones, S. (1998) Aluminium P/M MMC materials pose welding problems. *Metalwork News*, **685**, 10 – 12.
32. Vishnyakov, L.R., Oniskova, N.P., Romashko, I.M. *et al.* (1996) Technological mastering of composite materials of Al–SiC system. *Tekhn. Legkikh Splavov*, **3**, 64 – 69.
33. Ahearn, J.S., Cooke, C., Fishman, S.G. (1982) Fusion welding of SiC-reinforced Al composites. *Metal Construction*, **40**, 192 – 197.
34. Staufer, H., Nowak, M. (1998) GTA and GMA welding of particle reinforced aluminium. In: *Proc. of INALCO–98 7th Int. Conf. on Joints in Aluminium at TWI*. Abington, Cambridge, 15 – 17 April.
35. Klehn, R., Eagar, T.W. (1993) Joining of 6061 aluminium matrix/ceramic particle reinforced composites. *WRC Bulletin*, Vol. 385. New York.
36. Lugcheider, E., Burger, W., Broioch, U. (1997) Development and characterization of joining techniques for dispersion-strengthened alumina. *Welding J.*, **9**, 349 – 355.
37. Arun Junai, A., Botter, H., Brak, C.A. (1991) Diffusielassen van Al–SiC metal-matrix compositen. *Lastechnick*, **1**, 20 – 23.
38. Wang Guoging, Niu Jitai, Zhao Feng (1990) Diffusion bonding of SiC whisker reinforced aluminium composites. *J. Harbin Inst. of Technology*, **1**, 126 – 128.
39. Niu, J.T., Liu, L.M., Zhai, J.P. *et al.* (2000) Study on diffusion welding of aluminium matrix composite. *Acta Metallurgica Sinica (English Letter)*, **1**, 12 – 17.
40. Bushly, R.S., Scott, V.D. (1995) Joining of particulate silicon carbide reinforced 2124 aluminium alloy by diffusion bonding. *Mater. Sci. and Techn.*, **8**, 753 – 758.
41. Liu, L.M., Niu, J.T., Lai, Z.H. *et al.* (2000) Effects of diffusion welding parameters on joint strength of SiC/6061 Al composite. *Acta Metallurgica Sinica (English Letter)*, **1**, 201 – 204.
42. Partridge, P.G., Dunford, D.V. (1991) The role of interlayers in diffusion bonded joints in metal-matrix composites. *J. Mater. Sci.*, Vol. 26, 2255 – 2258.
43. Urena, A., Gomez de Salazar, J.M., Escalera, M.D. *et al.* (1994) Soldadura por diffusio de una allacion de aluminio (AA2124) reforzada con monocristales de SiC, mediante intermediarios de Al–Li (AA8090). *Review Soldadura*, **3**, 69 – 74.
44. Partridge, P.G., Shepherd, M., Dunford, D.V. (1991) Statistical analysis of particulate interface lengths in diffusion bonded joints in a metal-matrix composite. *J. Mat. Sci.*, Vol. 26, 4953 – 4960.
45. Zarapin, Yu.L., Chichenov, N.A., Chernilevskaya, N.G. (1991) *Composite materials manufacture by plastic working*. Refer. Book. Moscow: Metallurgia.
46. Lienet, T.J., Baeslack, W.A. (III), Ringnalda, J. *et al.* (1996) Inertia-friction welding of SiC-reinforced 8009 aluminium. *J. Mater. Sci.*, Vol. 31, 2149 – 2151.
47. Devletian, J.H. (1987) SiC/Al metal-matrix composite welding by capacitor discharge process. *Welding J.*, **6**, 33 – 39.

INFLUENCE OF ISOLATED INNER DEFECTS ON FRACTURE RESISTANCE OF WELDED JOINTS ON ALUMINIUM-LITHIUM ALLOYS

T.M. LABUR
The E.O. Paton Electric Welding Institute, NASU, Kyiv, Ukraine

ABSTRACT

The effect of discontinuities (isolated inner defects) in welded joints of high-strength aluminium alloys 1421 and 1460 was studied. The nature of change of the alloy mechanical properties and fracture toughness was established, depending on the presence of pores and oxide film inclusions in them. It is shown that oxide film inclusions at the same relative dimensions, as those of the pores, have a greater effect on welded joint properties.

Key words: *fusion welding, aluminium-lithium alloys, weld metal, isolated welding defects, pores, oxide film inclusions, mechanical properties, fracture resistance*

Deviations from the specified modes of welding aluminium alloys, often found in practice, result in formation of inner defects in welds, namely pores and oxide film inclusions. Large-sized defects are eliminated by repair welding. Fine isolated defects, as a rule, remain in welds, causing a local increase of stresses. Oxide films are considered among crack-like defects. The influence of the latter on strength is mainly evaluated in terms of fracture mechanics. Presence of isolated pores in the weld is less hazardous, as they do not result in brittle fracture of the metal. They, however, reduce the cross-sectional area, and, thus lower the joint strength. In critical situations defects can initiate brittle cracking.

Information on the influence of defects on welded joint performance, using fracture mechanics criteria, is scarce [1 – 3], and mostly concerns welded joints on medium-alloyed steels. The scope of such data for high-strength alloys is also limited. Nonetheless, it is known from publications that with the increase of the metal strength properties, its sensitivity to stress raisers becomes higher, especially at low temperatures. Therefore, studying the features of weld metal behaviour in high-strength Al–Li alloys, containing oxide film inclusions and pores, as well as determination of the influence of defects on welded joint performance and establishing admissible dimensions of inner defects in items of alloys 1421 and 1460, is an urgent problem. These are exactly the alloys demonstrating a higher susceptibility to formation of processing defects, namely alloy 1421 — to porosity and alloy 1460 — to oxide film inclusions [1]. Moreover, they are used in aerospace engineering components, operating in extremal conditions, therefore studying the influence of isolated defects on welded joint performance, is very important.

The field of application of fracture mechanics for calculation of admissible operational conditions or defect sizes, depends on the defect size, the reduction of which results in the stress intensity factor, K_{1c}, the main fracture resistance characteristic, being no longer invariant [4]. On the other hand, high-strength aluminium alloys mostly fail under load, exceeding the alloy yield point, and after extensive plastic deformation has been achieved [5]. Influence of defects on the change of fracture resistance was evaluated using the values of nominal breaking stress $\sigma_{br.def}$ and specific work of crack propagation ($SWCP_{def}$), obtained on Kahn samples [4]. These indices correlate quite well with value K_{1c} [6].

Butt joints of alloy 1421 were made using 2 mm filler wire Sv-AMg63 (Al–6.3Mg) and those of alloy 1460 — using Sv-1217 (Al–10Cu) wire. The procedure of preparation of 6 mm thick aluminium sheets and their welding modes were typical for argon-arc process of joining high-strength aluminium alloys [2]. The presence of defects was first detected on filmograms and etched sections from the weld root side. In the final form defect dimensions were determined more precisely on sample fractures after testing by axial and off-center tension. Relative size of the above defects in welds was calculated as the ratio of the cross-sectional area taken up by a unit defect S_{def} to the area that is the difference between the nominal section of tested sample S_s and studied defect area $S_{def}/(S_s - S_{def})$. Welded joint strength and nominal breaking stress at off-center tension were determined from $P/(S_s - S_{def})$ ratio, where P is the maximal load, at which an unstable crack propagation is found. The mean values of strength, ductility and fracture resistance were calculated by the results of testing five samples of welded joints, that had an approximately equal number of inclusions of oxide films and pores. The influence of pores was studied on welded joints of alloy 1421, and that of oxide films — on joints of alloy 1460.

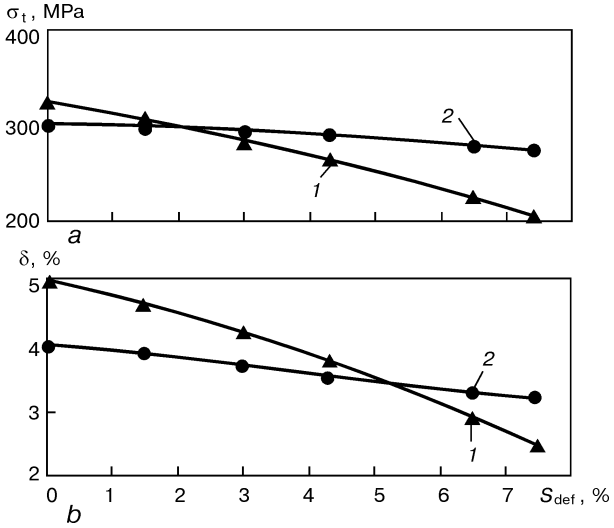

Figure 1. Dependence of strength σ_t (*a*) and ductility δ (*b*) of aluminium alloy welded joints on the size of processing defects S_{def}: *1* — oxide films; *2* — pores

Analysis of the derived data indicates that isolated pores, the area of which is equal to about 1 – 2 %, lower the strength, compared to sound samples of welded joints, just by 3 – 5 % (to 283 – 297 MPa). Ductility is reduced by 10 %, and the mean value of relative elongation is 3.8 %. The above regularity is clearly seen in Figure 1. In the presence of isolated inclusions of oxide film, that take up an area equivalent to that of the pores (1 – 2 %), their adverse effect on weld metal strength and ductility is more pronounced. Strength is lowered by 10 – 15 %, and relative elongation — by 20 – 25 %, compared to sound joints.

Increase of defect size to 5 % relative to the area of working cross-section of the sample, leads to further lowering of welded joint mechanical properties. The degree of adverse influence of oxide film inclusions is higher, than that of the pores. Relative elongation of the metal of such welds, at which the metal susceptibility to plastic deformation is manifested, decreases by 30 to 50 % in the presence of pores, and 2.0 to 2.5 times, if the welded joints contain isolated inclusions of oxide film.

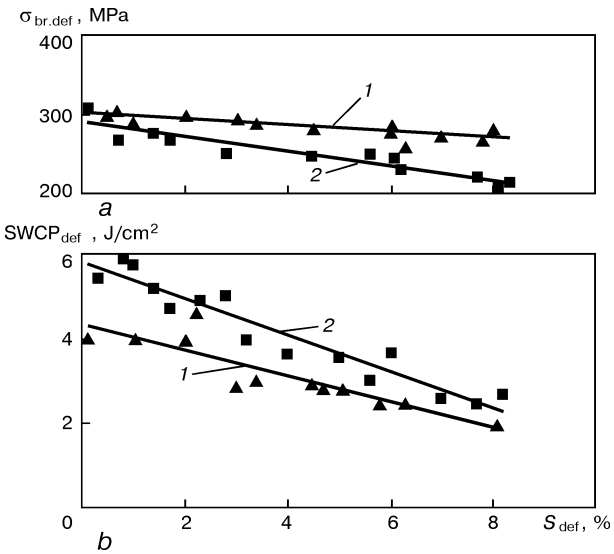

Figure 2. Influence of the size of processing defects, namely oxide film inclusions (*2*) and pores (*1*) on $\sigma_{br.def}$ (*a*) and $SWCP_{def}$ (*b*)

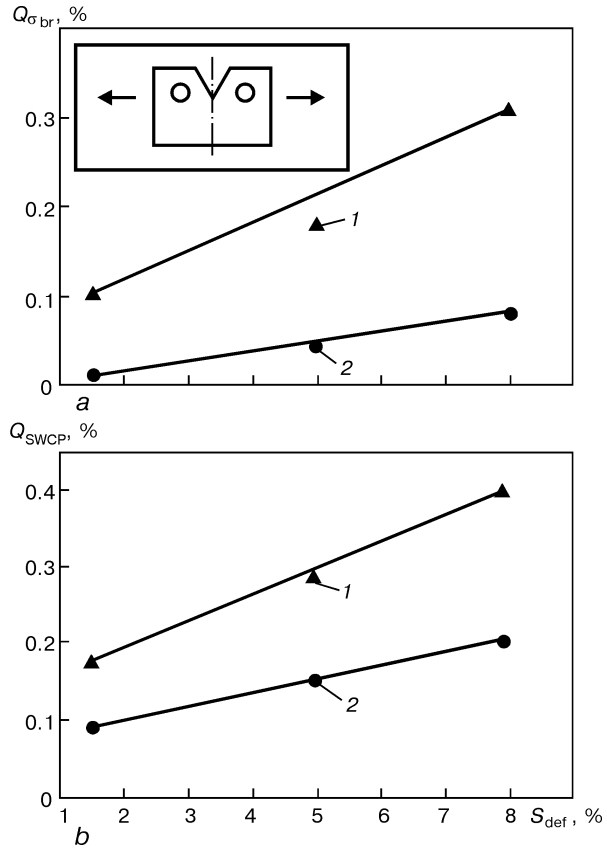

Figure 3. Sensitivity of aluminium alloy welded joints, depending on the kind and size of processing defects (designations of curves *1, 2* as in Figure 1)

A similar influence of the studied defects was also found in evaluation of the parameters of fracture resistance, namely nominal breaking stress $\sigma_{br.def}$ and $SWCP_{def}$ (Figure 2). An isolated pore of up to 2 % of the area of the sample working cross-section, does not have any significant influence on $\sigma_{br.def}$ level, its average value being 300 MPa. $SWCP_{def}$ value decreases by 10 – 15 %, compared to that of a sound welded joint, to 7 J/cm^2 on average. Presence of oxide film inclusions of the same size, has a stronger adverse influence on the joint fracture resistance. Value $\sigma_{br.def}$ of joints with oxide inclusions is by 15 – 20 % smaller, than in samples with pores of the same size. Increase of individual defect size to 8 %, leads to lowering of $\sigma_{br.def}$ by 13 – 20 (pores) and by 30 – 50 % (oxide film inclusions). Average values of nominal breaking stress of alloys 1421 and 1460 are equal to 278 and 255 MPa, respectively. $SWCP_{def}$ is reduced 1.5 or 2.0 times, depending on defect type (pores and oxide films). The found deterioration of the mechanical properties and fracture resistance of welded joints is due to the impact of defects solely as stress raisers, as they have been eliminated from the design cross-sectional area of the samples.

Considering the non-uniform influence of the studied defects, sensitivity *Q* of weld metal of aluminium

alloys 1421 and 1460, containing inclusions of oxide films or pores of equivalent size (Figure 3), was determined. The impact of the considered defects on the nominal breaking pressure was compared, using equation

$$Q = \sigma_{br} - \sigma_{br.def}/\sigma_{br}.$$

A similar approach was used also for $SWCP_{def}$:

$$Q = (SWCP - SWCP_{def})/SWCP.$$

As shown by the calculation results, oxide film inclusions have a 1.5 to 2.0 times stronger influence on the metal in the defect vicinity, than pores of equivalent dimensions (Figure 3). A marked deterioration of the properties of welded joints containing them, is indicative of the high degree of stress concentration. With the increase of the oxide film inclusion size, the tempo of properties deterioration increases 2 to 4 times (Figure 3). The found differences in the nature of the film and pore impact are attributable to their physical nature, as well as geometrical dimensions. The pore size was equal to tenth fractions of a millimeter (from 0.1 to 0.3 mm), and the oxide film thickness in most cases was equal to thousandth and ten thousandth fractions of a millimeter (from 1.10^{-6} up to 1.10^{-2}).

Analysis and generalisation of experimental results indicate that the limit size of the oxide film is 3 %, and that of the pores is 5 % of the working cross-section. The studied welded joints failed in the area, where the defect is located. With smaller defect sizes, the samples failed in the base metal.

CONCLUSIONS

1. Presence of isolated inner defects in welds on high-strength Al–Li alloys 1421 and 1460, equal to 1 – 2 % of the working cross-section area, lowers the values of strength and relative elongation, as well as fracture resistance of the metal. Oxide film inclusions lower the strength by 10 to 15 %, and relative elongation by 20 to 25 % (in the case of pores these values are 3 – 5 and 10 %, respectively, compared to sound samples).

2. Defects of the relative size of up to 5 % limit the plastic deformability of welded joint metal by 30 – 50 % in the case of pores and 2 times in the case of oxide film inclusions. Increase of the size of oxide inclusions up to 8 % of the working cross-section area, results in a marked lowering of the ductility level (by 20 – 25 % at axial tension) and of the nominal breaking stress (by 30 – 40 % at off-center tension). In joints with pores, these values are lowered by 15 – 20 %, compared to sound welds. Oxide film inclusions have a 2 – 3 times stronger influence on crack propagation energy, than pores of equivalent dimensions, which should be taken into account in developing the technology of welding critical components and structures of alloys 1421 and 1460.

3. Limit size of the defects encountered in welded joints of high-strength Al–Li alloys, can be not more than 5 % of the working cross-section area (for joints with pores) or 3 % (for oxide films).

REFERENCES

1. Rabkin, D.M. (1986) *Metallurgy of fusion welding aluminium and its alloys*. Kyiv: Naukova Dumka.
2. Ishchenko, A.Ya. (1991) Welding light alloys and metallic composite materials. *Avtomaticheskaya Svarka*, **6**, 26 – 31.
3. Kishkina, S.I. (1981) *Fracture resistance of aluminium alloys*. Moscow: Metallurgia.
4. Khertsberg, R.V. (1989) *Deformation and fracture mechanics of structural materials*. Moscow: Metallurgia.
5. (1986) *Static strength and fracture mechanics of steels*. Ed. by V. Dal, V. Anton. Moscow: Metallurgia.
6. Kobayashi, T. (1982) Strength and fracture of aluminium alloy. *J. of Light Metal Welding and Construction*, **10**, 539 – 552.

CHARACTER OF DIFFUSION OF CARBON WITHIN THE CONTACT ZONE IN THERMAL-PRESS ELECTRO-HYDROPULSE WELDING

L.Yu. DEMIDENKO and **N.A. ONATSKAYA**
Institute of Pulse Research and Engineering, NASU, Mykolaiv, Ukraine

ABSTRACT

It is shown that thermal-press electro-hydropulse welding of tubes to tube sheets results in formation of two bands in the contact zone — the carburized one on the tube side and the decarburized one on the tube sheet side. It has been found that formation of these bands is caused by directed diffusion of carbon, induced by residual tangential stresses with different signs, which are formed in elements being welded.

Key words: *thermal-press electro-hydropulse welding, pressure welding, tube, tube sheet, electro-hydropulse pressing-in, contact zone, diffusion, residual tangential stresses, carburized and decarburized bands*

The use of thermal-pressure electro-hydropulse (TPEHP) welding for joining tubes to tube sheets allows an increase in reliability and durability of heat exchangers operating at high pressures and temperatures under thermal cycling conditions, as well as under vibration, impact and other alternating loads [1]. This method is a modification of pressure welding with preheating, although it differs from the other known ones in that workpieces in a heated state are not affected by external pressure. This role is partially played by a residual contact pressure formed as a result of pressing-in of a tube into the tube sheet [2]. Therefore, the TPEHP process possesses certain physical peculiarities leading to creation of conditions for formation of welded joints by the technology which substantially differs from the traditional technology of solid-state welding of metals.

Analysis of differences of the technology of making welded joints by pressure welding [3] from the TPEHP welding process shows that the above peculiarities are related mostly to the use of electro-hydropulse pressing-in [4]. In particular, this is attributable to a much higher deformation of the mating surfaces, as compared with that observed during diffusion bonding, and to formation of the residual contact pressure between these surfaces. According to [3], during diffusion bonding the applied pressure hardly leads to macroscopic plastic deformation and changes in size of workpieces being joined. In TPEHP welding, owing to pressing-in, the residual plastic compression of the surfaces joined (expansion of tubes after making of initial gap) is several tenths of a millimeter. Tightness formed between the tube and the tube sheet is likely to prevent penetration of air between them during heating, i.e. this creates conditions preventing oxidation of the surfaces welded, similar to those occurring in auto-vacuum welding [5]. The fact that residual tangential stresses of opposite signs, i.e. compressive in the tube and tensile in the tube sheet, are formed in the contact zone as a result of pressing-in may play a certain role in formation of metallic bonds between the tube and the tube sheet during TPEHP welding. According to [6], this is one of the factors which enhance the diffusion processes. Pressing-in and heating to a welding temperature allow a rather intensive diffusion of atoms through the interface, provided that no external pressure is applied.

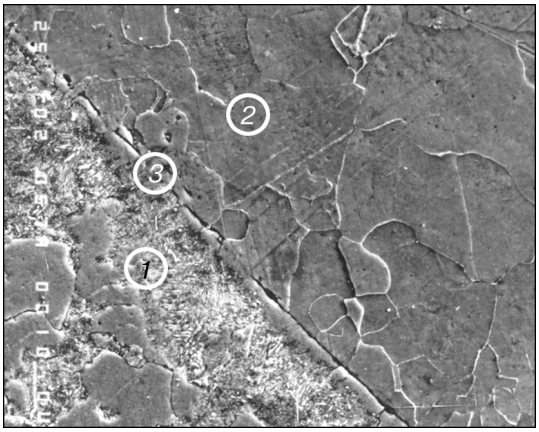

Figure 1. Microctructure of the pearlitic band in the interface zone of the TPEHP welded joint between tube and tube sheet: *1* — tube with the pearlitic band; *2* — tube sheet; *3* — interface (×1000)

The purpose of this work consisted in establishing the character of diffusion in the zone of contact of tubes with tube sheets during TPEHP welding, allowing for the peculiarities of distribution of residual stresses.

Metallography of the zone of the TPEHP welded joint between the tube and the tube sheet of low-carbon steel St.3 (C — 0.14 – 0.22; Mn — 0.3 – 0.6; Si — 0.05 – 0.17 wt.%) after annealing at a temperature of T_{an} = 900 °C for 35 min revealed that a carburized (pearlitic) band 18 – 40 μm wide was formed near the interface on the side of the tube, and a relatively wide (200 – 400 μm) decraburized band was formed in the tube sheet (Figure 1). It is characteristic

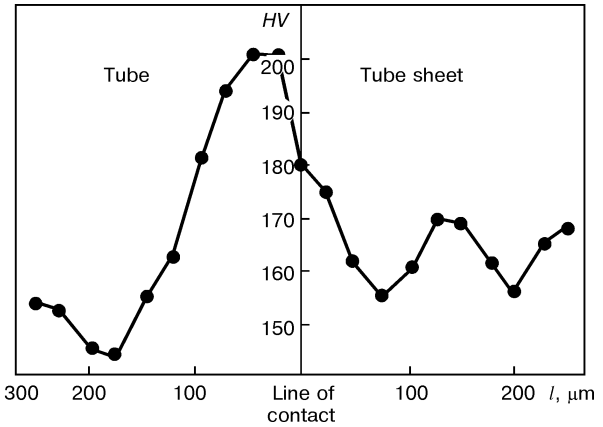

Figure 2. Distribution of microhardness in the contact and adjacent zones after annealing at T_{an} = 950 °C for 60 min

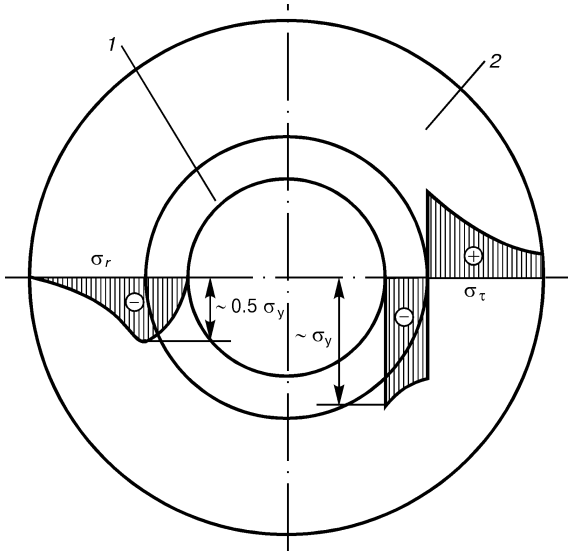

Figure 3. Characteristic diagrams of residual radial σ_r and tangential σ_τ stresses after elctro-hydropulse pressing-in of tube (*1*) into tube sheet (*2*)

that such a phenomenon occurs only at relatively high ($T_{an} \geq 900$ °C) heating temperatures, at which the diffusion processes are rather active [7]. In this case the formation of common ferritic grains takes place in the contact zone, which is accompanied by growth-through of the intergranular boundaries. The noted formation of the carburized and decarburized bands is proved by the data obtained by measuring microhardness in the contact and adjacent zones of welded joints (Figure 2). The measurement results are indicative of a redistribution of carbon, despite the absence of differences in its concentration in the initial state. Chemical composition of steel of the tube is as follows, %: C — 0.18; Mn — 0.52; Si — 0.06, and that of steel of the tube sheet — C — 0.17; Mn — 0.46; Si — 0.07.

The effect of diffusion redistribution of carbon in traditional pressure welding is described in [8]. In that case mobility of carbon was caused by difference in the concentration of alloying elements in contacting steels. It is likely that in TPEHP welding of tubes to tube sheets the redistribution of carbon is caused by the other factor, i.e. difference in signs of residual tangential stresses induced in the tube and tube sheet along the joint interface by the pressing-in operation, namely compressive stresses in the tube and tensile stresses in the tube sheet. It should be noted at this point that at relatively low radial stresses the residual tangential ones in the pressed-in tube have high values, close or even equal to yield stress (Figure 3). As it follows from [6], compression of metal results in its vacancy oversaturation, which causes the diffusion flows from the surrounding zones, directed to the compression side. Also, the rate of diffusion of carbon is known to be by several orders of magnitude higher than that of other elements, iron in particular [8]. This creates prerequisites for an increase in the concentration of carbon in a compressed interface region of the tube, namely for formation of the pearlitic band (see Figure 2). Considering the above-stated, we might say that TPEHP welding is characterized by an extra factor which intensifies the kinetics of the process of formation of a welded joint between the tube and the tube sheet at a relatively low contact pressure.

To prove the version of formation of the pearlitic zone in a tube material and, accordingly, the presence of another peculiarity of TPEHP welding, special investigations were conducted on the TPEHP welded joints between tubes 16.0 × 2.5 mm in size and tube sheets 60 mm thick. Both elements made from low-carbon steel 20 (C — 0.17 – 0.24; Mn — 0.35 – 0.37; Si — 0.17 – 0.37 wt.%). For this, an intermediate nickel interlayer was deposited on the tube by a galvanic method. The expediency of such investigations is dictated by the fact that nickel prevents diffusion of carbon [8]; therefore, no pearlitic band should be formed in this case in the tube. To ensure the sufficient activity of the diffusion processes, the temperature of heat treatment was selected to be equal to 900 °C at a holding for 480 min.

Metallography and microprobe analysis were conducted using the JEOL X-ray microanalyser ISHA-733. Investigations of the contact zone yielded the expected result, namely no pearlitic band was formed

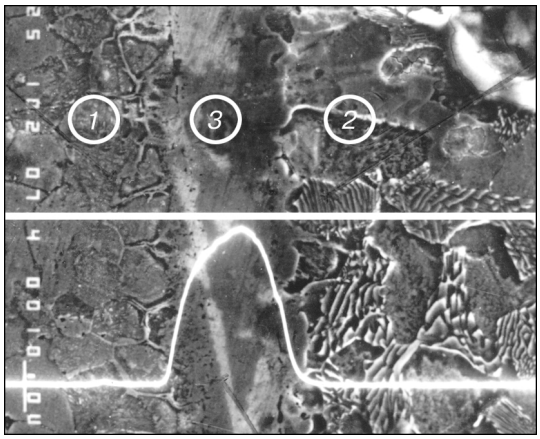

Figure 4. Microstructure of the contact and adjacent zones and distribution of nickel after TPEHP welding using a nickel interlayer: *1* — tube; *2* — tube sheet; *3* — nickel interlayer (×1000)

on the tube side; however, on the side of the tube sheet the concentration of pearlite increased to some extent, as compared with the initial one (Figure 4). In parallel, the microprobe analysis was carried out to study distribution of nickel along a line normal to the interface between the tube and the tube sheet (Figure 4), which fixed the absence of diffusion of nickel from the interlayer.

The results obtained showed that in TPEHP welding a one-sided directed diffusion of carbon took place through the interface from the tube sheet into the tube. This was caused by the presence of tangential stresses of different signs in workpieces welded. Therefore, TPEHP welding is characterized by the presence of an extra factor activating the process of formation of the welded joint, which compensates for the insufficiency of the contact pressure.

REFERENCES

1. Opara, V.S., Demidenko, L.Yu. (1996) Thermal-press welding — a radical way of increasing reliability of heat exchanging devices. *Tyazh. Mashinostroyeniye*, **10**, 23 – 26.
2. Opara, V.S., Yurchenko, E.S., Demidenko, L.Yu. (1992) Evaluation of the role of high-temperature collision in formation of a tube–tube sheet welded joint. *Avtomaticheskaya Svarka*, **8**, 15 – 16.
3. Kazakov, N.F. (1976) *Diffusion bonding of materials*. Moscow: Mashinostroyeniye.
4. Mazurovsky, B.Ya. (1980) *Electro-hydropulse pressing-in of tubes in tube sheets of heat exchanging devices*. Kyiv: Naukova Dumka.
5. Finkelshtein, M.L. (1978) *Diffusion bonding in liquid media*. Moscow: Metallurgia.
6. Karakozov, E.S., Ternovsky, A.P. (1984) Pressure welding: diffusion bonding. In: *Results of science and technology*, Series Welding, Vol. 16. Moscow: VINITI.
7. Karakozov, E.S. (1976) *Solid-state joining of metal*. Moscow: Metallurgia.
8. Livshits, L.S., Khakimov, A.N. (1989) *Welding metals science and heat treatment of welded joints*. Moscow: Mashinostroyeniye.

PECULIARITIES OF FORMATION OF FRICTION WELDED JOINTS BETWEEN COPPER AND ALUMINIUM

I.V. ZYAKHOR and S.I. **KUCHUK-YATSENKO**
The E.O. Paton Electric Welding Institute, NASU, Kyiv, Ukraine

ABSTRACT

Peculiarities of different types of friction welding of copper to aluminium, such as conventional, inertia and combined welding, are considered. Factors affecting formation of welded joints are analysed on the basis of experimental data. Conditions which determine formation and growth of the intermetallic interlayer in the joining zone are considered. Principles of control of the welding process to provide sound joints have been developed.

Key words: *conventional friction welding, inertia friction welding, technology, dissimilar joints, heating and forging stages, process parameters, pressure, rotation speed, upsetting, time of heating and deceleration, equipment, intermetallic interlayer, quality of a joint*

The necessity of joining copper to aluminium arises in the manufacture of current-conducting parts and units of electric machines, transformers, busbars of power-intensive plants, chemical engineering vessels and other items [1].

Friction welding is one of the efficient methods of making dissimilar joints, including between copper and aluminium. Such welding of metals, which are substantially different in their properties, has a number of peculiarities associated with different melting temperatures and thermal conductivities, as well as with a different effect of welding thermal conditions on the character of deformation of billets being joined. However, the highest differences are caused by chemical interaction of metals being joined, which leads to formation of a brittle intermetallic interlayer in the joining zone.

It is well-known [2 – 8] that to produce a quality welded joint it is necessary to minimize thickness of the intermetallic interlayer. Welding parameters recommended by different authors greatly differ from each other. The characteristic feature of conventional friction welding is application of a substantial forging pressure (p_f = 120 – 210 MPa) at the final stage of the process, which is required to remove the brittle intermetallic layer from the joint.

Available literature data on welding of copper to aluminium were obtained in conventional friction welding, which is characterized by a rapid forced termination of rotation. At the same time, using the inertia completion of the welding process makes it possible in many cases to optimize thermal-deformation conditions of formation of the joints, in particular in dissimilar combinations of many materials [9 – 12].

The work described in this article was aimed at comparison of conditions of formation of welded joints between copper and aluminium in two modifications of friction welding, i.e. conventional and inertia friction welding, as well as at development of the friction welding technology which would provide high me-

chanical and service properties of copper-aluminium transition pieces.

Copper M1 (GOST 859–78) and commercial aluminium AD1 (GOST 4784–74) in the form of billets with a diameter of 22 mm were used as the base materials. Investigations were conducted using the conventional friction welding machines MST-2001 and ST-120, and the inertia friction welding machine ST-100. The spindle rotation drive of the ST-120 machine is actuated from the DC motor with a controllable rotation frequency, which allowed the linear speed to be varied within wide ranges.

Linear speed v on the periphery of the billets welded was 0.5, 0.75, 1.0, 1.5, 2.0 and 2.5 m/s at the selected rotation frequencies. Pressure at the heating stage, p_h, was varied from 20 to 100, and that at the forging stage, p_f, was varied from 50 to 210 MPa. The process of heating the billets was regulated on the basis of heating upsetting varied from 1 to 15 mm. The time of the deceleration stage in conventional welding was 0.2 s. Technological parameters of inertia welding (initial rotation speed, moment of inertia of rotating masses) were set such that the specific energy input into the joint was 12.9 – 54.0 MJ/m^2.

During the process the following welding parameters were registered by the N145 oscillograph: temperature at three points of the joint (on the periphery T_p, at the centre T_c and at a distance of $0.5R$ from the centre, T_d); heating and forging pressures p_h and p_f; upsetting during heating and forging Δl; heating time t_h and heat release capacity N; moment of friction M measured using a device equipped with strain gauges [13]. Temperature of the contact zone was measured with chromel-alumel thermocouples (wire diameter 0.2 mm). As in welding of aluminium to copper the latter is hardly deformed, the thermocouple junction was caulked directly into the plane of friction of the copper billet.

Strength of welded joints was determined by mechanical tensile tests according to GOST 1497–73 and impact toughness tests according to GOST 9454–78. It should be noted that standard testing methods do not allow a comprehensive evaluation of the quality of the joints in dissimilar metals [14]. Tensile tests are insufficiently sensitive to the presence of a transition intermetallic layer and, as well as impact toughness and static bending tests, do not enable estimation of the quality of the entire welded joint. This made it necessary to conduct extra full-scale tests of welded

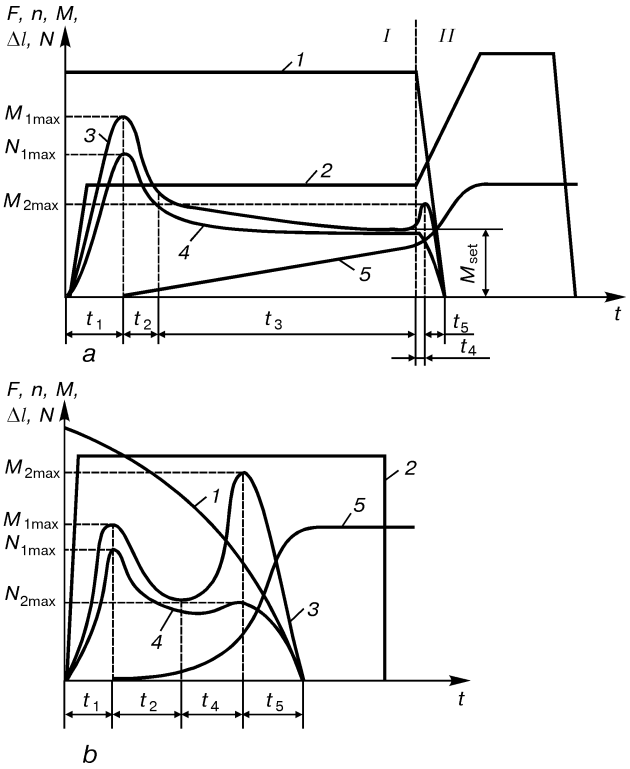

Figure 1. Typical oscillograms of the processes of conventional (*a*) and inertia (*b*) friction welding: *1* — rotation frequency n; *2* — axial force F; *3* — moment M; *4* — capacity of heat release at the joint N; *5* — upsetting Δl (contraction); *I* — heating stage; *II* — forging stage

joints as a whole (after flash removal) to impact bending. This testing method widely used by foreign investigators [4, 14] for evaluation of the quality of dissimilar joints is much more sensitive to the presence of lack of penetration and transition intermetallic layers, as compared with other standard methods.

Typical oscillograms of variations in main technological parameters of conventional and inertia friction welding are shown in Figure 1.

As established by measurement of temperature of the contact zone (Table 1), under the investigated process conditions the temperature quite rapidly (for 0.4 – 1.2 s) reaches a value of 350 – 500 °C, i.e. the point at which chemical interaction of the metals welded can occur, which is accompanied by reactive diffusion and formation of intermetallic compounds. The process of heating of a joint is non-uniform (Figure 2, *a*). Maximum of heat released in the initial period of friction, corresponding to time t_1, was fixed in the circular zone located at a distance from the

Table 1. Results of measurement of maximum temperature of the copper–aluminium contact zone at different values of deposition pressure and rotation speed (diameter of billets 22 mm, pressure during heating 50 MPa, heating allowance 8 mm)

p_h, MPa	v = 0.75 m/s			v = 1.5 m/s			v = 2.0 m/s		
	T_p, °C	T_c, °C	T_d, °C	T_p, °C	T_c, °C	T_d, °C	T_p, °C	T_c, °C	T_d, °C
25	445	395	440	500	475	505	515	490	510
40	450	400	450	505	480	510	520	485	510
60	400	360	390	495	450	490	510	480	505
80	360	320	345	460	435	460	495	450	490
100	340	305	330	430	410	435	480	445	480

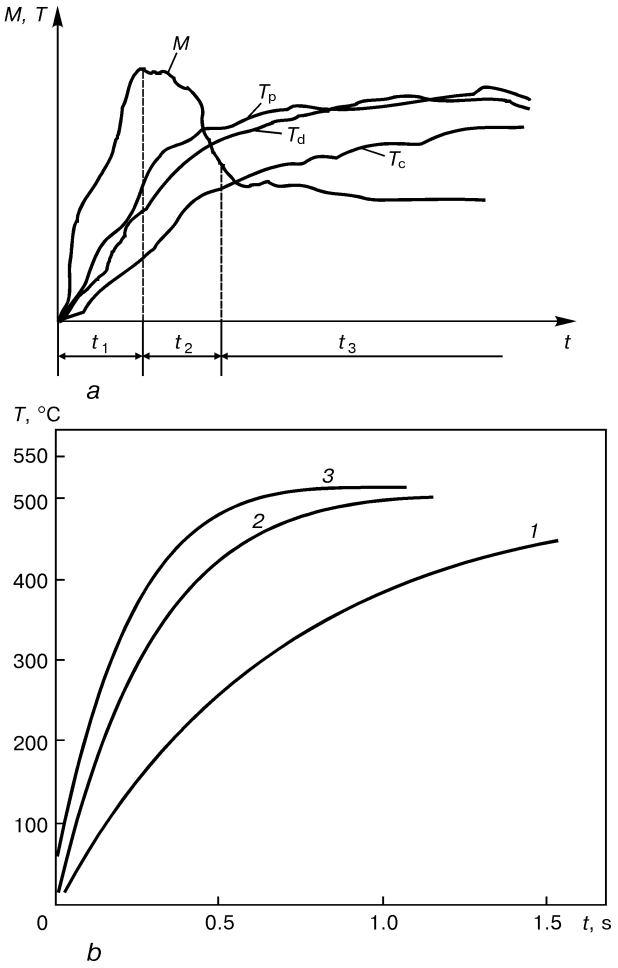

Figure 2. Time variations in the friction moment and temperature (*a*) at different points of the contact surface and maximum temperature in the contact zone (*b*) at p_h = 40 MPa and v = 0.75 (*1*), 1.5 (*2*) and 2.0 (*3*) m/s

periphery of the billets to $0.5R$ from the centre, and minimum was fixed at the centre. The difference between maximum and minimum heating temperatures in this period amounts to 150 °C. The next period of friction with a duration of t_2 is characterized by redistribution of heat release on the friction surface, i.e. an intensive increase in temperature is fixed at the centre of the joint, whereas on the periphery and at a distance of $0.5R$ from the centre its growth slows down. The third period of heating with a duration of t_3 is characterized by levelling of the temperature at all points of the joint, i.e. the process stabilizes and

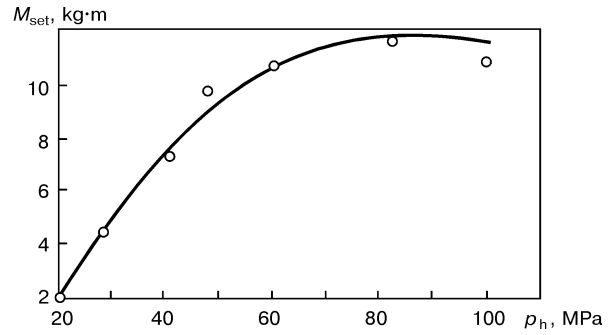

Figure 3. Dependence of the set friction moment upon pressure during heating

further heating occurs almost uniformly (quasi-stationary heating).

Analysis of oscillograms taken at different parameters of the welding process shows that the intensity of energy release in different phases of the process depends upon the rotation speed and axial force during heating. An increase in the rotation frequency is accompanied by an increase in the intensity of growth of temperature (Figure 2, *b*) and its levelling across the entire section. An increase in the axial force leads to an increase in height of the first and second peaks of the friction moment (M_{1max} and M_{2max} in Figure 1, *a*), set value of the friction moment M_{set} (Figure 3) and rate of plastic deformation (upsetting). This is accompanied by a decrease in time of the stage of quasi-stationary heating t_3 (see Figure 1, *a*).

Processing of the data of mechanical tests showed the following. Joints of a satisfactory quality can be produced over a wide range of variations in the welding process parameters: linear speed from 0.75 to 2.50 m/s, heating pressure from 25 to 100 MPa, forging pressure not less than 150 MPa and heating allowance from 1.5 to 8.0 mm. However, an important factor is not so much the value of individual parameters as their combination, providing an optimal value of the rate of axial deformation at the heating stage, on condition that time or upsetting at this stage is strictly regulated. Joints with the best strength and ductility values were produced at v = 1.5 – 2.0 m/s and p_h = 40 – 70 MPa, which provide the axial deformation rate equal to 5.5 – 8.0 mm/s.

Investigations of macrostructure of the joints revealed no pores, voids or lack of fusion at the interface (Figure 4, *a*, *b*). Results of measurement of microhardness using the LECO-400 instrument at a minimum load of 0.1 N and loading time of 10 s are shown in Figure 5. Thickened contact layers of aluminium with microhardness HV 340 – 360 MPa are 1.5 – 2.0 mm thick. Adjoining these layers is a region of recrystallized base metal with microhardness HV 320 – 330 MPa. Fracture in tensile tests occurs as a rule in this region (Figure 4, *c*). Structure of the joining zone on the side of copper (Figure 6, *a*, *b*) comprises finer grains, as compared with the base metal, and flattened grains formed as a result of cold-working, while the zone of increased hardness is 40 μm wide.

Metallography of sound joints produced by conventional friction welding reveals the presence of a transition layer, which is non-uniform across the section (Figure 6, *c*, *d*). Results of electron probe X-ray analysis (Figure 7, *a*) using the «Cameca» device SX-50 (probe diameter 1 μm) show that the phase corresponding to intermetallic compound $CuAl_2$ dominates in the transition layer, and that the zone of volumetric interaction, based on solid solution α + + $CuAl_2$, is formed on the side of aluminium.

Mechanical properties of bimetal joints are known to depend upon the thickness of the intermetallic transition layer [1, 2]. It was established as a results of combined analysis of results of metallography and

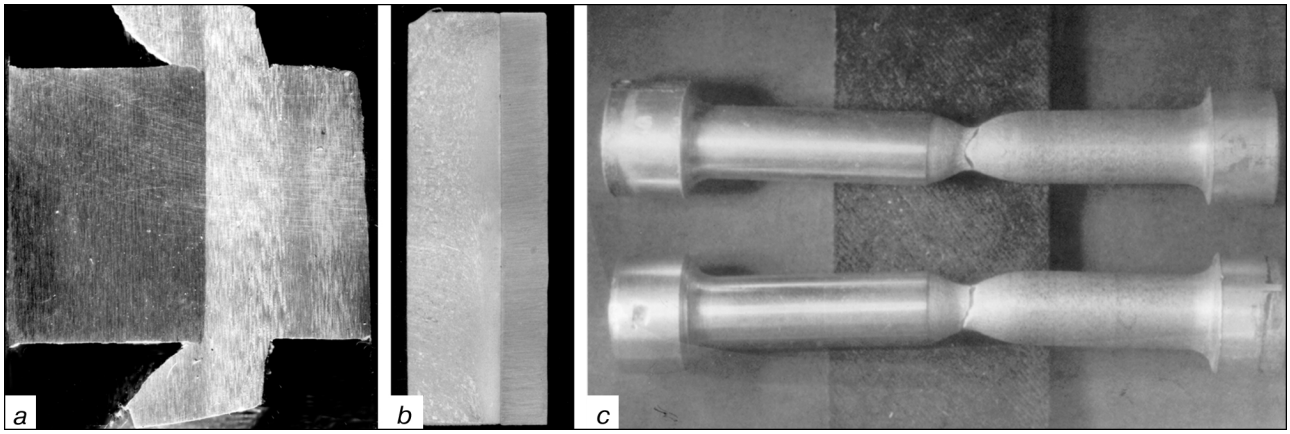

Figure 4. Joint produced by conventional friction welding using forming devices: *a* — general view; *b* — macrostructure (×4) (reduced by 3/5); *c* — after tensile tests

data of mechanical tests of copper-aluminium transition pieces that the joints with the transition layer not more than 2 μm thick have high ductile properties in impact bend tests. In tensile tests the positive results (fracture in the aluminium base metal) were obtained at a much thicker transition layer (approximately up to 10 μm thick).

It was shown that thickness of the intermetallic transition layer in a joint depends upon the combination of technological parameters of the welding process. An increase in thickness of the intermetallic interlayer is promoted by an increase in the linear speed and heating allowance, as well as by a decrease in the heating and forging pressures. Therefore, to minimize thickness of the intermetallic layer it is necessary to reduce the time of heating at a preset combination of other process parameters.

However, as proved by numerous experiments, it is impossible to produce joints with high values of mechanical properties and eliminate formation of the intermetallic layer in the conventional friction welding process. This is associated with peculiarities of the final stage of the welding process, i.e. quick braking of rotation. Interpretation of oscillograms of this process shows that stopping of rotation at the final stage leaves behind the application of the preset forging force, which results in a rapid decrease in temperature of the mating surfaces and temperature gradient within the plastic deformation zone. At the time of the quasi-stationary heating stage limited by time-temperature conditions of formation of intermetallics, the attempts to ensure the required degree of plastic deformation at the final stage of the process fail even at an application of the substantial forging pressure. Therefore, the time of the heating stage in conventional welding should be sufficient for a certain temperature gradient to form in the joining zone. In this case, again, it is impossible so far to avoid formation of the intermetallic interlayer.

Besides, the range of variations in the main technological parameters, at which the possibility exists of producing sound welded joints, is determined in many respects by dynamic characteristics of the axial force and rotation drives of the involved welding equipment. Thus, the joints with a bending angle of 90° were produced using the standard welding machine MST-2001 at a forging pressure p_f of not less than 200 MPa, and using the ST-120 machine at a forging pressure of 150 MPa. Owing to a higher response of the axial force drive of the ST-120 machine,

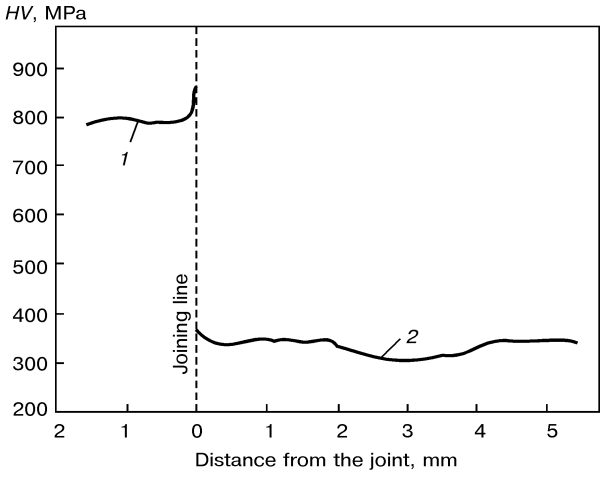

Figure 5. Variations in microhardness in the copper (*1*) to aluminium (*2*) joining zone

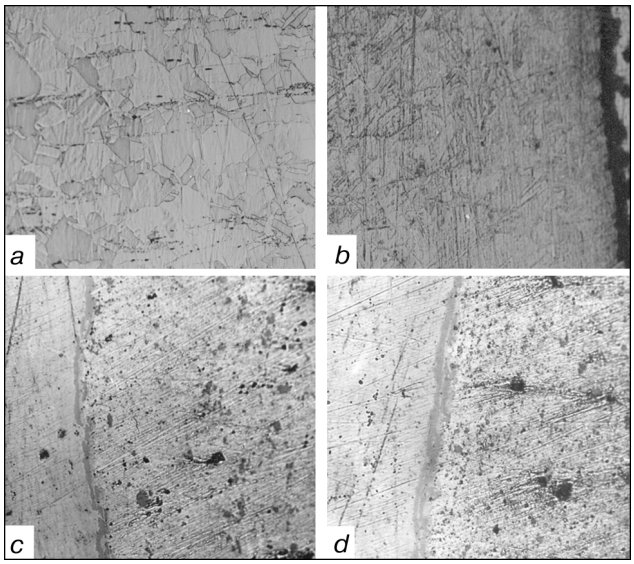

Figure 6. Microstructure of the welded joint: *a* — base metal (copper); *b* — copper near the interface, (×100); *c* — at the centre; *d* — on the periphery (×625) (reduced by 2/5)

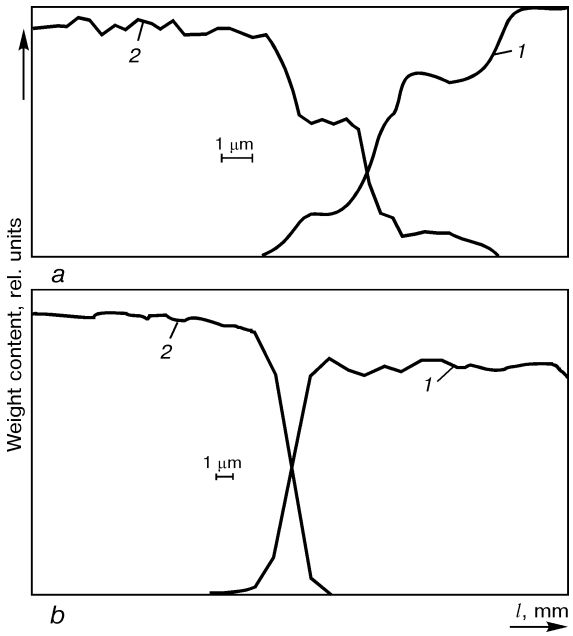

Figure 7. Distribution of copper (*1*) and aluminium (*2*) across the interface in conventional (*a*) and inertia (*b*) friction welding

it is possible to speed up the application of the forging force and ensure a higher degree of plastic deformation in the joining zone at a lower value of the forging pressure. To produce sound welded joints using the MST-2001 machine, it is necessary to increase the time of heating and the forging force, combined with the use of forming devices (see Figure 4, *a*). It is likely that peculiarities of the involved welding equipment can account for substantial differences in parameters of welding of copper-aluminium transition pieces as given by different investigators [2 – 8].

Analysis of oscillograms of the process of inertia welding of copper to aluminium allowed the following peculiarities to be revealed. The third phase (of quasi-stationary heating) is hardly formed, and value of the second peak of the friction moment is much in excess of that occurring in conventional welding. Formation of the second peak on the curve of the friction moment (see Figure 1, *b*) is attributable to the fact that a decrease in the rotation speed is accompanied by a decrease in the temperature field gradient and an increase in the depth of the zone in which a heat release occurs as a result of the deformation flow of metal and break of the metallic bonds.

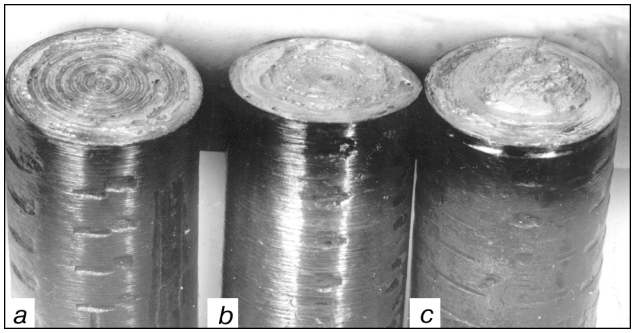

Figure 8. Fracture surfaces of welded joints produced at a heating pressure of 25 (*a*), 40 (*b*) and 50 (*c*) MPa

Table 2. Results of mechanical impact bending tests of copper–aluminium joints produced by inertia friction welding (diameter of billets 22 mm, pressure 65 MPa)

Inertia moment of rotating masses, I, kg·m²	*Rotation frequency, n, rpm*	*Specific energy, e_s, MJ/m²*	*Bending angle to fracture, degr*
0.4	1500	12.9	5
0.4	1700	16.7	15
0.4	2000	23.1	90 (no fracture)
0.4	2200	27.9	90 (no fracture)
0.4	2500	36.0	65
0.6	2500	54.0	20

It was established that at the final stage of deceleration the friction process is accompanied by deep levelling and displacement of the friction surface towards the aluminium billet. Fractures of the joints produced under low pressures (less than 60 MPa) exhibit the presence of an aluminium layer (Figure 8) transferred to the surface of the copper billet, 0.1 – 0.5 mm thick. This is indicative of the fact that strength of the formed bonds at the stage of an inertia completion of the heating process is higher than strength of the aluminium base metal, these bonds covering the entire nominal surface of the billets joined.

Therefore, the joints are finally formed between the aluminium billet and the aluminium layer transferred to the surface of the copper billet. As in inertia welding, unlike conventional welding, the axial force at the final stage of the process is applied to the rotating billets, this ensures also the high intensity and degree of localization of deformation in the contact zone. Owing to the combined action on a softened metal layer by the axial force and friction moment, the sound joints can be produced at a much lower axial force than in conventional welding. Under the inertia welding conditions with a specific energy of 23 – 28 MJ/m^2, the minimum pressure, under which it is possible to ensure high strength and ductility values of the welded joints, was decreased to 65 MPa (Table 2, Figure 9). It should be noted that at a single-step application of the axial force, characteristic of inertia welding, the process of formation of the joints is less dependent upon the dynamic characteristics of the force drive of the involved welding equipment.

Metallography of sound welded joints failed to detect the transition layer containing an intermetallic phase. The method of making microsections was employed to get a deeper insight into the joining zone. In this case a joint was cut out at an angle α to the joining plane, so that thickness of the joining line was visually increased by a factor of $1/\sin\alpha$.

Electron probe X-ray analysis proved the absence of the intermetallic phase at the interface of the joints produced by inertia friction welding. Curves of distribution of copper and aluminium (see Figure 7, *b*) comprise no bends characteristic of the joints with a constant or variable composition; instead, mutual dif-

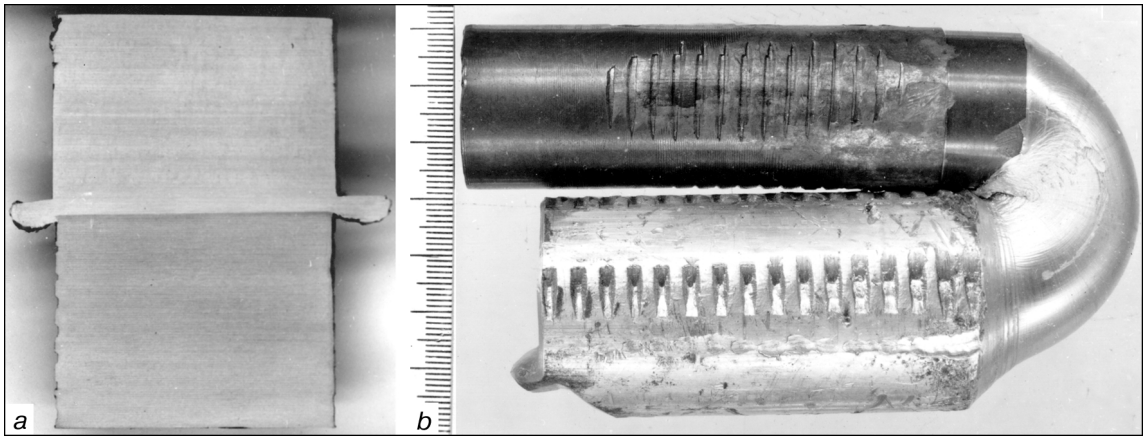

Figure 9. Joints produced by inertia friction welding: *a* — as-welded; *b* — after mechanical tests

fusion of copper and aluminium to a depth of down to 3 μm takes place in this zone. The transition zone formed in this case is most favourable.

The data of metallography and electron probe X-ray analysis evidence that in inertia welding under optimal conditions the growth of the intermetallic phase was limited and, owing to localization of deformation in the contact zone, the joints had a dispersed structure without the intermetallic layer.

The following basic principles for controlling the process of formation of friction welded joints in transition pieces between copper and aluminium were developed on the basis of the obtained results:

• precise portioning of energy input into the joint at the heating stage. This is achieved through controlling the basic technological parameters which provide conditions under which the thermal welding cycle is not in excess of the time-temperature conditions of formation of the intermetallic interlayer in the joining zone;

• regulation of the dynamics of variation of the rotation speed in welding: high values at the initial stage and gradually decreasing to zero at the final stage. This creates conditions for intensification and localization of plastic deformation in the contact zone;

• cyclogram of application of the axial force and specific values of the forging pressure should be determined with allowance for dynamic characteristics of the force drive of a welding machine employed.

CONCLUSIONS

1. To produce sound joints by conventional friction welding, it is necessary to use an optimal combination of technological parameters to ensure the certain rate of axial deformation during heating, and set the forging pressure with allowance for dynamic characteristics of the axial force drive of a welding machine.

2. The intermetallic transition layer was detected in sound joints produced by conventional friction welding. High mechanical properties of the joints are achieved at the presence of the transition layer to up to 2 μm thick.

3. By setting the appropriate parameters of the inertia friction welding process the growth of the intermetallic phase can be limited to its initial stages. In this case, a dispersed structure containing no intermetallic layer is formed in the joining zone owing to intensification of deformation and its localization along the contact surface.

4. Displacement of the friction surface towards an aluminium billet takes place during inertia friction welding at the final stage of heating. This is indicative of the fact that strength of the bonds formed in the joining zone is higher than strength of the aluminium base metal at the final stage of welding.

5. Established was the feasibility of decreasing pressure at the final stage of the process of inertia friction welding, as compared with conventional friction welding.

REFERENCES

1. Ryabov, V.R. (1983) *Welding of aluminium and its alloys to other metals*. Kyiv: Naukova Dumka.
2. Lebedev, V.K., Chernenko, I.A., Vill, V.I. *et al*. (1987) *Friction welding*. Refer. Book. Leningrad: Mashinostroyeniye.
3. Shternin, L.A., Prokofiev, S.N. (1961) Friction welding of aluminium to steel and copper. *Svarochnoye Proizvodstvo*, **11**, 30 – 32.
4. Ellis, C.R., Nicholas, E.D. (1975) Determination of a procedure for making friction welds between electrical grade aluminium and tough pitch copper. *Weld. Res. Int.*, **1**, 1 – 32.
5. Kreye, H., Reiners, G. (1986) Metallurgical aspects and application of friction welding. In: *Proc. of Int. Conf. on Advances in Welding Science and Technology,* Gatlinburg, USA, 18 – 22 May.
6. Braun, E., Braun, I.J. (1969) *The joining of copper to aluminium by friction welding*. UKAEA Res. Group Rep.
7. Yilbas, B.S., Safin, A.Z., Kahraman, N. *et al*. (1995) Friction welding of St–Al and Al–Cu materials. *J. Mater. Proc. Techn.*, **49**, 431 – 443.
8. Aritoshi, M., Okita, K., Enjo, T. *et al*. (1993) Friction welding of copper sintered alloy to pure aluminium. *Transact. Jap. Weld. Soc.*, **1**, 50 – 56.
9. Lebedev, V.K., Chernenko, I.A. (1992) Friction welding. In: *Welding and Surfacing Rev.*, vol. 2, part 4. Harwood A.P.
10. Kuchuk-Yatsenko, S.I. (1998) State-of-the-art and prospects of development of friction welding. In: *Proc. of Int. Conf. on Welding and Related Technologies for the 21-st century*, Kyiv, November. Kyiv: PWI.
11. Chernenko, I.A., Zyakhor, I.V. (1999) Friction welding of dissimilar metals and alloys. *Svarshchik*, **1**, 10 – 12.
12. Kuchuk-Yatsenko, S.I., Zyakhor, I.V. (1999) Friction welding of dissimilar metals. In: *Proc. of Symp. on Exploiting Solid State Joining*, 13 – 14 Sept., Cambridge. Abington: TWI.
13. Lebedev, V.K., Litvin, L.V., Dyshlenko, A.T. *et al*. (1986) Determination of the friction moment in inertia welding by the value of angular acceleration. *Avtomaticheskaya Svarka*, **8**, 31 – 33.
14. Ellis, C.R., Nicholas, E.D. (1976) Mechanical testing of dissimilar metal friction welds. *Weld. Res. Int.*, **2**, 1 – 22.

INTERACTION OF COPPER WITH INSOLUBLE IMPURITIES UNDER CONDITIONS OF PULSED DEFORMATION IN PRESSURE WELDING

V.V. ARSENYUK
NASU, Kyiv, Ukraine

ABSTRACT

Interaction of copper with gallium, carbon and inert gases under conditions of vacuum percussion, magnetic-pulse and explosion welding has been investigated. Formation of solid solutions in the mass transfer zone is noted. Dependencies of the concentration of a dissolved element and its penetration depth upon the temperature, strain rate and welding method have been determined.

Key words: *percussion welding, magnetic-pulse welding, explosion welding, mass transfer, dissolution of elements, solid solution*

It is reported [1] that phase composition in vacuum percussion welding of dissimilar metals differs from the equilibrium one, for example, in that no intermetallic compounds are formed in welding copper to tin or aluminium, or in occurrence of solubility between copper to molybdenum, i.e. two insoluble metals with a crystalline structure of atoms in the form of a cubic lattice. Moreover, addition of atoms of an inert gas to metal results in their redistribution and migration during subsequent pulsed treatment or pressure welding, which leads to formation of the metal–inert gas solid solution [2]. Therefore, in welding dissimilar structural materials which have, as a rule, a complex chemical phase composition, it is necessary to allow for the probability of formation of compounds of elements which earlier were considered insoluble. In this connection, of interest is to investigate peculiarities of interaction of copper with elements which are not dissolved in it under equilibrium conditions, i.e. metal and light element, in the case of superposition of pulsed deformations in various pressure welding processes.

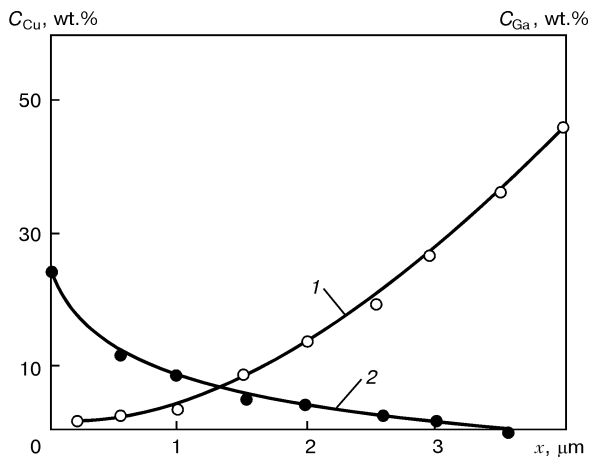

Figure 1. Distribution of gallium in copper (*1*) and copper in gallium (*2*) in the case of explosion welding at $\dot{\varepsilon} = 5 \cdot 10^6$ s^{-1}

The processes of redistribution of atoms and variation in phase composition in the zone of contact of copper and different elements in vacuum percussion welding [3], magnetic-pulse welding [4] and explosion welding [5] were investigated by the methods of layer-by-layer radiometry, X-ray diffraction and electron probe X-ray analysis and Moessbauer spectroscopy.

Gallium was selected as an insoluble metal impurity, as its crystalline structure (orthorhombic lattice) drastically differs from the face-centered lattice of copper. In addition, for equilibrium conditions, at no solubility of copper in gallium, the latter penetrates into copper, being dissolved in it up to 20 % [6].

The investigations performed showed that all the welding methods under consideration resulted in mutual penetration of these elements and formation of solid solutions. However, solubility of gallium in copper in pulsed deformation performed by the methods described in [3 – 5] over the entire range of strain rates ($\dot{\varepsilon} = 1 \cdot 10 - 5 \cdot 10^6$ s^{-1}) is higher than that of copper in gallium. Therefore, the absence of solubility under equilibrium conditions does not impede solubility under loading, although the amount of a dissolved material in this case is lower than in the case where metals are dissolved under the isothermal holding conditions. Changing from percussion welding to magnetic-pulse and explosion welding, i.e. an increase in the strain rate, is accompanied by an increase in the penetration depth and concentration of a dissolved material. At $\dot{\varepsilon} \cong 5 \cdot 10^6$ s^{-1} (in the case of explosion welding) the penetration depth amounts to 4 mm and the concentration is 48 %, i.e. composition of the weld metal is close to the equiatomic one (Figure 1).

Interaction of copper with carbon over a temperature range of 300 to 1073 K under percussion compression also results in formation of a solid solution, although under equilibrium conditions there is no contact between these elements. However, under conditions of magnetic loading at a strain rate of about

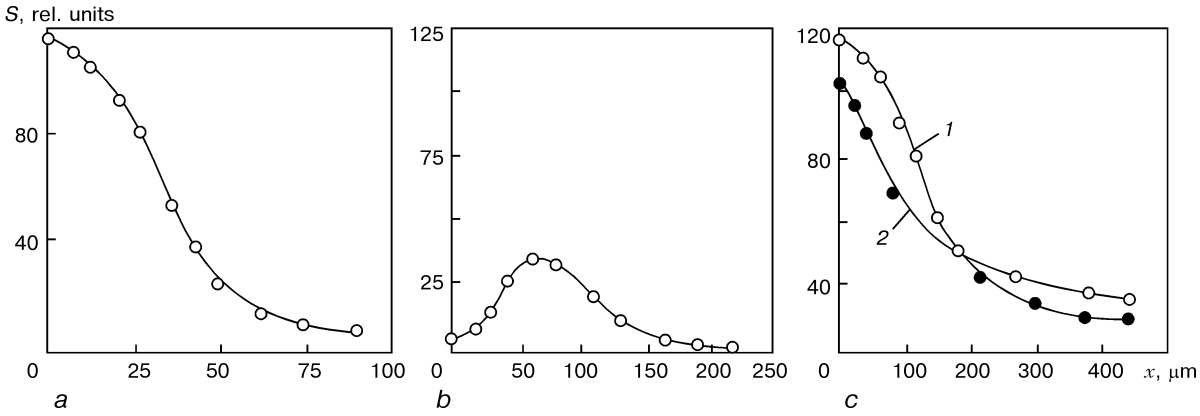

Figure 2. Distribution of ^{14}C in copper after pulsed loading: *a* — vacuum percussion welding at $\dot{\varepsilon} = 25$ s^{-1}; *b* — magnetic-pulse welding at $\dot{\varepsilon} = 2 \cdot 10^3$ s^{-1}; *c* — explosion welding at $\dot{\varepsilon} = 3 \cdot 10^5$ (*1*) and $7 \cdot 10^5$ (*2*) s^{-1}

25 s^{-1} during heating to 1073 K, in iron containing ^{14}C, which is in contact with copper, carbon penetrates into copper to a depth of about 80 – 90 μm (Figure 2, *a*), and its concentration is about 1 %. It should be taken into account in this case that iron atoms simultaneously migrate into copper. In turn, this favours dissolution of carbon in the copper matrix, as was the case of stationary isothermal conditions [7, 8]. To eliminate the effect of this factor, the experimental design was changed so that copper and carbon interacted in their pure forms. Glow-discharge treatment of copper in methane labelled with ^{14}C is one of the methods of adding carbon into copper. Subsequent pulsed loading at $\dot{\varepsilon} \cong 1 \cdot 10^3 - 1 \cdot 10^4$ s^{-1} at a temperature of 373 – 673 K leads to redistribution of carbon atoms and their transfer to a depth of about 200 μm (Figure 2, *b*). In this case the concentration of carbon in the subsurface copper layers amounted to 5 %. An increase in the strain rate to $(3 - 7) \cdot 10^5$ s^{-1} in the case of explosion welding favours penetration of carbon into copper to a larger depth, amounting to about 400 μm (Figure 2, *c*). It should be noted that penetration of carbon into copper occurred during the loading process in the case of a direct contact of copper with graphite containing ^{14}C.

Analysis of the data in Figure 2 showed that an increase in the strain rate is accompanied by penetration of carbon, similarly to elements that have mutual solubility, to an increasingly large depth. Besides, an increase in temperature from room one to 400 °C at a strain rate of $1 \cdot 10^3$ s^{-1} and higher has almost no effect on the extension of the mass transfer zone. At lower rates of plastic strain, an increase in temperature, at which pressure pulse welding is performed, is accompanied by some increase in the penetration depth and rate of migration of carbon into copper.

Further treatment of the resulting joints showed that redistribution of dissolved gallium and carbon, as well as an increase in their total penetration depth occurred in subsequent deformation without heating. However, an increase in temperature during the process of isothermal heating or static deformation favours escape of the elements investigated from solid solution. This is accompanied by formation of intermetallic compounds of copper with gallium and a graphite interlayer.

Therefore, pulsed deformation during the pressure welding process leads to dissolution in copper of those elements which did not interact with it under equilibrium conditions. But as the thus formed solid solutions are metastable, they disintegrate during subsequent treatment to bring phase composition of metal into correspondence with the constitutional diagram.

REFERENCES

1. Arsenyuk, V.V., Gertsriken, D.S., Mazanko, V.F. *et al.* (1997) Peculiarities of phase formation in interaction of metals under the effect of pulsed loading. *Metal. i Obrob. Mater.*, **2**, 21 – 25.
2. Arsenyuk, V.V., Gertsriken, D.S., Mazanko, V.F. *et al.* (1997) Migration of atoms in a metastable iron-argon solid solution. *Dopovidi NANU*, **8**, 108 – 112.
3. Larikov, L.N., Falchenko, V.M., Mazanko, V.F. *et al.* (1974) Peculiarities of mass transfer in solid-state welding of armco iron. *Avtomaticheskaya Svarka*, **5**, 19 – 21.
4. Larikov, L.N., Falchenko, V.M., Gertsriken, D.S. *et al.* (1978) On the mechanism of effect of a magnetic pulse field on mobility of atoms in iron and aluminium. *Doklady AN SSSR*, **2**, 312 – 314.
5. Kudinov, V.M., Koroteev, A.Ya. (1978) *Explosion welding in metallurgy*. Moscow: Metallurgia.
6. Drits, M.E., Bochvar, N.R., Guzej, L.S. *et al.* (1979) *Binary and multicomponent copper-based systems*. Moscow: Nauka.
7. Geguzin, Ya.Ye. (1979) *Diffusion zone*. Moscow: Nauka.
8. Gusak, A.M., Mazanko, V.F., Tomashevsky, N.A. *et al.* (1992) Peculiarities of phase formation under pulsed effect. *Metallofizika*, **3**, 33 – 36.

INTERACTION OF RESIDUAL STRESSES IN THE ZONES OF STRESS CONCENTRATORS AND FATIGUE CRACKS

V.A. BRODOVOJ, O.I. GUSHCHA, A.Z. KUZMENKO and **P.P. MIKHEEV**
The E.O. Paton Electric Welding Institute, NASU, Kyiv, Ukraine

ABSTRACT

It has been experimentally demonstrated that interaction of residual stresses in the zones of stress concentrators and fatigue cracks induced by cyclic loading with stresses induced by strengthening treatment results in the formation of a residual stress field that differs essentially from the initial one.

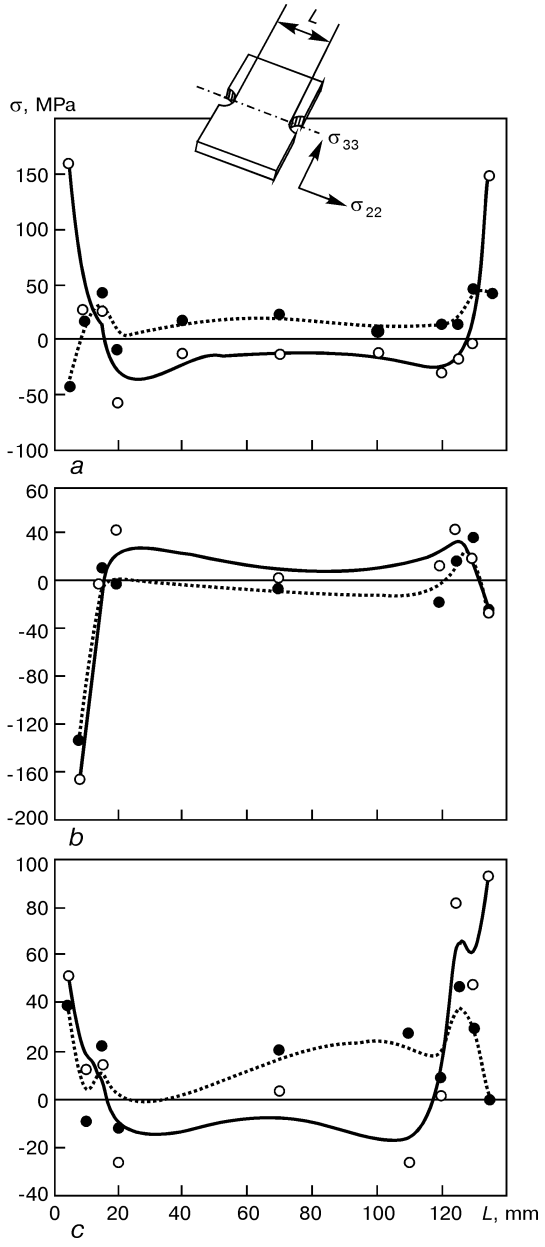

Figure 1. Diagrams of residual stresses in the St.3 sample with stress concentrators $\alpha_\sigma = 2.48$: *a* — after 10 cycles of loading by cyclic compression; *b* — after high-frequency peening of the concentrator zone; *c* — after 10 cycles of repeated compression loading (here and in Figure 2 ● — σ_{22} and ○ — σ_{33})

Key words: *residual stresses, stress concentration, fatigue resistance, fatigue crack, strengthening treatment*

Different strengthening methods are employed to increase cyclic strength of welded joints. Methods based on inducing compressive residual stresses in the stress concentrator zones are very efficient in this respect [1]. These stresses interact with residual welding stresses and with stresses caused by cyclic loading in the concentrator and fatigue crack zones. This results in the formation of a new field of residual stresses, which can essentially differ from its initial stress components in sign, level and distribution character. In turn, these residual stresses undergo changes and redistribution under cyclic loading.

Therefore, in evaluation of the effect of residual stresses on the processes of initiation and distribution of fatigue fracture, it is necessary to take into account the interaction and kinetics of these stresses.

The work described in this article considered interaction of residual stresses in the stress concentrator and fatigue crack zones with compressive residual stresses additionally induced by high-frequency peening and spot heating, as well as their kinetics under the effect of external cyclic loading.

A sample of killed steel St.3 (C — 0.14 – 0.22; Mn — 0.3 – 0.6 wt.%; Fe — balance) measuring 14 × × 160 × 240 mm with the concentrators in the form of side holes (Figure 1) was loaded by axial from-zero cyclic compression. The theoretical stress concentration coefficient was $\alpha_\sigma = 2.48$. Maximum stresses of the nominal loading cycle were –120 MPa. Residual stresses σ were measured by a nondestructive acoustic method [2].

The level of residual stresses in the stress concentrator zone was stabilized after the first several loading cycles [3]. Therefore, stresses formed after 10 loading cycles were fixed (Figure 1, *a*). As it can be seen from the Figure, cyclic compression resulted in the formation of a biaxial field of tensile residual stresses (σ_{22} — transverse and σ_{33} — longitudinal stresses) with a maximum value of 150 MPa. Then the sample was successively treated in holes by high-frequency peening. This treatment resulted in relief of tensile stresses and formation of biaxial residual compressive stresses in the concentrator zones (Figure 1, *b*), whose maximum val-

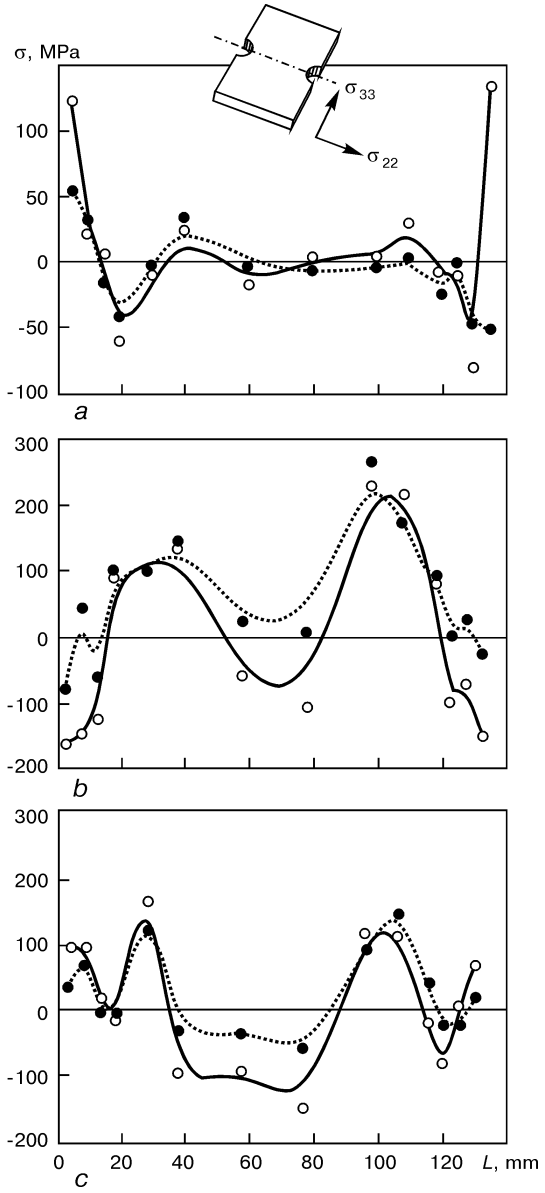

Figure 2. Diagrams of residual stresses in the St.3 sample: *a* — after 10 cycles of pulsed compression loading; *b* — after treatment by spot heating; *c* — after 10 cycles of repeated compression loading

ues were in excess of −160 MPa. Some differences in the measured values of stresses at different edges of the sample are attributable to the sequence of treatment of the concentrators.

The sample was repeatedly loaded by cyclic compression. Allowing for a strengthening effect of previous loading of the sample, the maximum stress values of a nominal loading cycle were a bit higher than the previous ones and amounted to −125 MPa. The repeated 10 cycles of compression loading again resulted in the formation of a biaxial field of tensile residual stresses in the concentrator zones. Their maximum value was 90 MPa.

Another sample of a similar type was loaded by pulsed compression $\sigma_{min} = -125$ MPa. After 10 cycles a field of biaxial residual stresses (Figure 2, *a*) with a maximum level of 125 – 130 MPa was fixed in the concentrator zones.

Then the sample was subjected to treatment by spot heating. Heating spots were located at a distance of

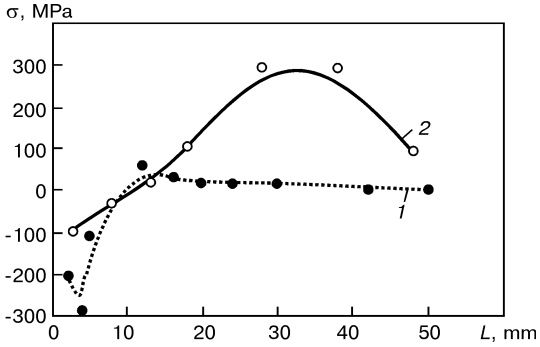

Figure 3. Kinetics of a longitudinal component of residual stresses in the crack zone: *1* — sample with crack in the initial state; *2* — after spot heating

35 mm from the end of each concentrator. The sample was heated first on one side and then, after complete cooling, on the other side. Under the effect of treatment the level and distribution of residual stresses were essentially changed (Figure 2, *b*). Biaxial compressive stresses with maximum values of −160 MPa were formed in the concentrator zones. Tensile residual stresses with a maximum level equal to the yield point of steel were formed in the heating zones.

Tensile residual stresses (Figure 2, *c*) were again formed in the concentrator zones after 10 cycles of repeated loading by cyclic compression. Their maximum values were 70 – 100 MPa. The level of stresses at the heating points was decreased to some extent.

At initiation of a fatigue crack the field of residual stresses was formed in the zone of its apex. Figure 3 shows diagrams of residual stresses formed in the fatigue crack zone also after spot heating of the sample. The sample of steel St.3 measuring $12 \times 250 \times 700$ mm had at its centre a stress concentrator in the form of a through hole with notches that initiated fatigue cracks. The sample was loaded by the from-zero cyclic tension using the TsDM-200Pu machine. Maximum compressive residual stresses in the fatigue crack zone initially reached the yield point of steel. After the spot heating treatment the values of compressive stresses at the crack apex decreased to −100 MPa.

Therefore, residual stresses formed under the effect of cyclic loading in the stress concentrator and fatigue crack zones interact with stresses artificially induced by the methods of strengthening treatment. Such an interaction was fixed both at the stage of initiation of a fatigue fracture and after formation of the fatigue crack. This results in the formation of the fields of residual stresses, which in many respects determine resistance of materials and welded joints to initiation and propagation of fatigue cracks.

REFERENCES

1. Trufiakov, V.I., Mikheev, P.P., Kudryavtsev, Yu.F. (1995) Fatigue strength of welded structures. Residual stresses and strengthening treatments. In: *Welding and Surfacing Rev.*, vol. 3. Harwood A.P.
2. Gushcha, O.I., Makhort, F.G. (1976) Acoustic method of estimation of biaxial residual stresses. *Prikladn. Mekhanika*, **10**, 32 – 36.
3. Brodovoj, V.A., Mikheev, P.P., Gushcha, O.I. (2001) Some regularities in formation of residual stresses in zones of a stress raiser and fatigue crack at cyclic loading. *The Paton Welding Journal*, **2**, 8 – 11.